

# An ab Initio Study on the Allene–Isocyanic Acid and Ketene–Vinylimine [2 + 2] Cycloaddition Reaction Paths

Joanna E. Rode<sup>†</sup> and Jan Cz. Dobrowolski<sup>\*,†,‡</sup>

Industrial Chemistry Research Institute, 01-793 Warsaw, 8 Rydygiera Street, Poland, and National Institute of Public Health, 00-725 Warsaw, 30/34 Chełmska Street, Poland

Received: September 8, 2005; In Final Form: November 22, 2005

The reaction paths of [2 + 2] cycloadditions of allene ( $\text{H}_2\text{C}=\text{C}=\text{CH}_2$ ) to isocyanic acid ( $\text{HN}=\text{C}=\text{O}$ ) and ketene ( $\text{H}_2\text{C}=\text{C}=\text{O}$ ) to vinylimine ( $\text{H}_2\text{C}=\text{C}=\text{NH}$ ), leading to all the possible 14 four-membered ring molecules, were investigated by the MP2/aug-cc-pVDZ method. In the two considered reactions, the 2-azetidinone ( $\beta$ -lactam) ring compounds were predicted to be the most stable thermodynamically in the absence of an environment. Although 4-methylene-2-azetidinone is the most stable product of the ketene–vinylimine cycloaddition, its activation barrier is higher than that for 4-methylene-2-iminoxetane by ca. 6 kcal/mol. Therefore, the latter product can be obtained owing to kinetic control. The activation barriers in the allene–isocyanic acid reactions are quite high, 50–70 kcal/mol, whereas in the course of the ketene–vinylimine cycloaddition they are equal to ca. 30–55 kcal/mol. All the reactions studied were found to be concerted and mostly asynchronous. Simulation of the solvent environment (toluene, tetrahydrofuran, acetonitrile, and water) by using Tomasi's polarized continuum model with the integral equation formalism (IEF-PCM) method showed the allene–isocyanic reactions remained concerted, yet the activation barriers were somewhat higher than those in the gas phase, whereas the ketene–vinylimine reactions became stepwise. The larger the solvent dielectric constant, the lower the activation barriers found. The lowest-energy pathways in the gas phase and in solvent were confirmed by intrinsic reaction coordinate (IRC) calculations. The atoms in molecules (AIM) analysis of the electron density distribution in the transition-state (TS) structures allowed us to distinguish pericyclic from pseudopericyclic from nonplanar–pseudopericyclic types of reactions.

## Introduction

The discovery of penicillin in 1929,<sup>1</sup> a  $\beta$ -lactam-containing antibiotic, remains one of the most important contributions of science to humanity as, from the beginning, the antibiotics have been shown to act against bacterial infections.<sup>2</sup> Nowadays,  $\beta$ -lactams are the most widely employed family of antimicrobial agents accounting for 50% of the world's antibiotic market.<sup>3</sup> Of the many different families of  $\beta$ -lactam drugs now known, most have a fused bicyclic framework.<sup>4</sup> The discovery of monobactams<sup>5</sup> and nocardicins<sup>6</sup> has revealed that, to be antibacterial agents,  $\beta$ -lactams do not have to be fused bicyclic 2-azetidinone compounds.

Current applications of the 2-azetidinone unit molecules are much wider than just antibacterial agents. One of the most promising nonantibiotic uses of  $\beta$ -lactams is the inhibition of serine protease enzymes. Among the enzymes inhibited effectively by the  $\beta$ -lactam compounds are cytomegalovirus protease,<sup>7</sup> prostate specific antigen,<sup>8</sup> thrombin, and elastase,<sup>9</sup> which hold potential for the control of human cytomegalovirus, prostate and breast cancers, thrombotic episodes, and emphysema, respectively. 2-Azetidinones are also potent human leukocyte elastase<sup>10</sup> (HLE) and cholesterol absorption inhibitors.<sup>11</sup> Moreover, the  $\beta$ -lactam ring is utilized in commercial production of Taxol, a widely used anticancer drug.<sup>12</sup>

The discovery of monocyclic  $\beta$ -lactam antibiotics, arousing interest in nonantibiotic activity and use of the  $\beta$ -lactam ring as a synthetic building block, results in permanent interest in the synthesis of  $\beta$ -lactam ring compounds. Even if the aim is to synthesize the bicyclic antibiotics, the first step is to prepare the 2-azetidinone ring so it is suitably stereoconfigured at the C3 and C4 atoms.<sup>13</sup> Numerous methods of the  $\beta$ -lactam skeleton synthesis have been proposed.<sup>14</sup> Usually, the  $\beta$ -lactam ring is formed through either ketene–imine or isocyanic acid–olefin or allene cycloaddition. The former is known as the Staudinger reaction, discovered long before the biological activity and therapeutic value of the  $\beta$ -lactam moiety were established.<sup>15</sup> The cycloaddition of unsymmetrically substituted allenes to isocyanates provides a general access to synthetically useful  $\alpha$ -alkylidene- $\beta$ -lactams antibiotics of the penicillin type: carpetimycins,<sup>16</sup> asprenomycins,<sup>17</sup> and thienamicin.<sup>18</sup> Despite the synthetic importance of such a reaction, little has been reported on its mechanism and a number of literature considerations are often qualitative and contradictory. For example, the existence of an intermediate,<sup>19</sup> the classical Woodward–Hoffmann *supra*–*antra*,<sup>20</sup> and pseudoconcerted mechanisms were proposed.<sup>21,22</sup> The mechanism of the allene–isocyanic acid reaction, leading to 3-methylene- $\beta$ -lactam, was investigated by Cossio et al. at the HF/6-31G\* and MP2/6-31G\* levels.<sup>23</sup> The transition-state (TS) structures found were planar and corresponded to a concerted (one-step), yet asynchronous mechanism, namely,  $[\pi 2_s + \pi 2_a]$ .<sup>23</sup> However, the MP2/6-31+G\* calculations have shown that the inclusion of both electron correlation and diffuse

\* To whom correspondence should be addressed. Tel: +(48)-568-24-21. E-mail: Jan.Dobrowolski@ichp.pl or janek@il.waw.pl.

<sup>†</sup> Industrial Chemistry Research Institute.

<sup>‡</sup> National Institute of Public Health.

functions led to a nonplanar TS, and therefore, a [ $\pi 2_s + (\pi 2_s + \pi 2_s)$ ] mechanism was proposed instead of the [ $\pi 2_s + \pi 2_a$ ].<sup>24</sup> Reactions of unsubstituted allenes yielded 4-methylene- $\beta$ -lactams,<sup>23–25</sup> however, inclusion of substituents in the allene moiety yielded the 3-methylene isomers. The results were concordant with experimental findings. In experiments, allenes substituted by  $\pi$ -donor functional groups were used and only 3-methylene regioisomers were obtained. Inclusion of a solvent effect into the calculations has shown the energy profile to change completely with respect to that found in the gas phase: the reaction has become a stepwise (two-step) process.<sup>24</sup>

The ketene–imine Staudinger cycloaddition<sup>15</sup> has provided useful and economic entries to  $\beta$ -lactams, mainly due to the ready availability of both, Schiff's bases and ketenes.<sup>14</sup> According to the experimental results of Moore and co-workers,<sup>26</sup> the cycloaddition of ketene to imine is a two-step zwitterionic process rather than a concerted one. This was also confirmed by IR detection of a zwitterionic intermediate appearing in thermal reactions of ketene with imines followed by a detailed kinetic analysis by using low-temperature FTIR spectroscopy.<sup>27</sup> The first theoretical semiempirical and Hartree–Fock (HF) investigations confirmed these results: the reaction was found to be a stepwise process.<sup>28</sup> The ketene–imine cycloaddition mechanism toward 2-azetidinone seems to be solved unequivocally by Assfeld et al. and Truong.<sup>29</sup> It was shown that the solvent (1,4-dioxan,<sup>29a</sup> acetonitrile,<sup>29a</sup> or water<sup>29b</sup>) significantly stabilized the zwitterionic complex, consequently changing the topology of the free energy surface from the one-step in the gas phase to the two-step process.<sup>29</sup> As the polarity of the solvent increased, a greater stabilization of all the structures considered was observed.<sup>29a</sup> Furthermore, the solvent effect was found to lower the activation barrier by 4.5 kcal/mol in line with the previous experimental data.<sup>29b</sup>

Also, the ketene–vinylimine cycloaddition reaction could possibly yield 4-methylene- $\beta$ -lactams.<sup>25</sup> We demonstrated that out of the 11 possible products of such a reaction, 4-methylene- $\beta$ -lactam is the one most stable thermodynamically.<sup>25</sup> However, no other theoretical nor experimental paper has dealt with this reaction. On the other hand, we did not consider the mechanism of this reaction, and this seems to be desirable as the experimental findings report 2-iminooxetanes to be the main product of the catalyzed cycloaddition reaction of vinylimine with ketenes or aldehydes.<sup>30</sup>

In both isocyanic acid–allene and ketene–vinylimine reactions, 14 molecules could possibly form,<sup>25</sup> however, out of them, only the 3-methylene-2-azetidinone molecule is known.<sup>31</sup> Quite recently, the chemistry of azetin-3-ones has been reviewed,<sup>32</sup> and some halogen derivatives of 1,2-oxazetidines<sup>33</sup> and iminooxetanes<sup>34</sup> have been discovered and characterized.

The objective of this study is to investigate the allene–isocyanic and ketene–vinylimine [2 + 2] cycloaddition reaction paths leading to all possible four-membered ring products. To this aim, we have performed MP2/aug-cc-pVDZ calculations for the reactants, TS structures, and reaction products. Next, for the lowest-energy pathways, solvent environments were simulated by the IEF-PCM method. In the calculations, solvents of different dielectric permittivities were taken into account: toluene ( $\epsilon = 2.379$ ), tetrahydrofuran (THF,  $\epsilon = 7.58$ ), acetonitrile (36.64), and water (78.39). Although it was shown that water reacts immediately with ketenes<sup>35</sup> and isocyanates<sup>36</sup> yielding carboxylic or carbamic acids, we simulated a water environment to show energetic and geometrical tendencies with increasing dielectric permittivities.

Also, for the lowest-energy pathways, the mechanisms in the gas phase and in the solvents were confirmed by performing the intrinsic reaction coordinate (IRC) calculations. The atoms in molecules (AIM) analysis of critical points of the electron density in the TSs allowed us to find arguments for a distinction between pericyclic, pseudopericyclic, and nonplanar (NP)-pseudopericyclic types of reactions.

This paper is organized as follows: First, the energetics of the two [2 + 2] cycloaddition reactions in the gas phase are discussed. Next, the geometrical parameters, with special emphasis on the TSs, are analyzed. Then, the influence of solvents on the reaction energetics and geometrical parameters of the reaction components are modeled. Finally, reaction mechanisms are discussed in terms of AIM analysis of the TS structures.

## Calculations

All calculations were performed at the MP2/aug-cc-pVDZ level<sup>37,38</sup> which includes electron correlation effects and utilizes a large basis set containing both diffused and polarized functions. It was shown that HF theory usually overestimates barrier heights for chemical reactions and pure density functional theory (DFT) usually underestimates them.<sup>39</sup> On the other hand, it was shown by Cossio et al.<sup>24</sup> that inclusion of both electron correlation and diffuse functions enabled us to find proper, nonplanar, geometries of TS structures.

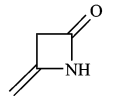
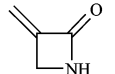
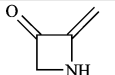
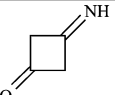
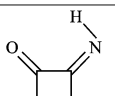
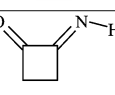
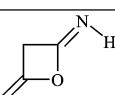
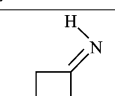
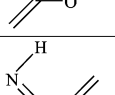
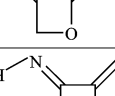
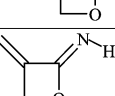
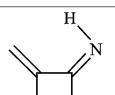
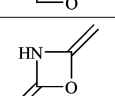
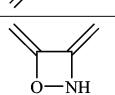
The TS structures were found by using the quadratic synchronous transit-guided quasi-Newton (QST3) method developed by Schlegel and co-workers, which uses a quadratic synchronous transit approach to get closer to the quadratic region around the TS and then uses a quasi-Newton or eigenvector-following algorithm to complete the optimization.<sup>40</sup> As for minimizations, it performs optimizations by default using redundant internal coordinates.<sup>41</sup>

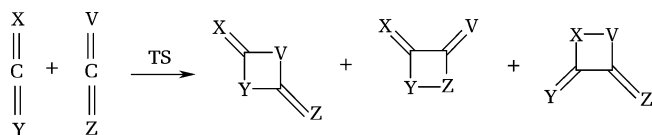
The influence of the solvent was studied for the low-energy profiles. To model the solute–solvent interactions, Tomasi's polarized continuum model with the integral equation formalism (IEF-PCM) was used.<sup>42</sup> In this procedure, the solvent is mimicked by a dielectric continuum with dielectric constant  $\epsilon$  surrounding a cavity with shape and dimension adjusted on the real geometric structure of the solute molecule. The latter polarizes the solvent which, as a response, induces an electric field (the *reaction field*) which interacts with the solute. In the IEF-PCM, the electrostatic part of such an interaction is represented in terms of an apparent charge density spread on the cavity surface.

Full geometry optimizations were performed both in the gas phase and in solvents. All stationary points (minima and TSs) were characterized as minima or transition structures by calculating the harmonic vibrational frequencies, using analytical second derivatives. Also, the low-energy pathways for the reactions running in a vacuum and in all solvents were confirmed by using the IRC method with mass-weighted coordinates.<sup>43</sup> Starting from the TS, the reactants and products are unequivocally identified.

For the lowest-energy TSs in the most different environments, gas and water, the atomic charges were calculated based on the method that fits the charges to reproduce the molecular electrostatic potential (MEP) at a number of points around the molecule.<sup>44</sup>

**TABLE 1: Schematic Structures, Molecule Numbering, Names of the Systems Studied, and the Reaction Types Leading to Them**

Structure	Numbering	Name	Obtained in reaction:
	1	4-methylene-azetidin-2-one (4-methylene-2-azetidinone)	1. allene+isocyanic acid 2. ketene+vinylimine
	2	3-methylene-azetidin-2-one (3-methylene-2-azetidinone)	allene+isocyanic acid
	3	2-methylene-azetidin-3-one (2-methylene-3-azetidinone)	ketene+vinylimine
	4	3-imino-cyclobutanone	ketene+vinylimine
	5	2-imino-cyclobutanone	ketene+vinylimine
	6	2-imino-cyclobutanone	ketene+vinylimine
	7	4-methylene-oxetan-2-ylideneamine (4-methylene-2-iminooxetane)	1. allene+isocyanic acid 2. ketene+vinylimine
	8	4-methylene-oxetan-2-ylideneamine (4-methylene-2-iminooxetane)	1. allene+isocyanic acid 2. ketene+vinylimine
	9	2-methylene-oxetan-3-ylideneamine (2-methylene-3-iminooxetane)	ketene+vinylimine
	10	2-methylene-oxetan-3-ylideneamine (2-methylene-3-iminooxetane)	ketene+vinylimine
	11	3-methylene-oxetan-2-ylideneamine (3-methylene-2-iminooxetane)	allene+isocyanic acid
	12	3-methylene-oxetan-2-ylideneamine (3-methylene-2-iminooxetane)	allene+isocyanic acid
	13	2,4-dimethylene-[1,3]oxazetidine	ketene+vinylimine
	14	3,4-dimethylene-[1,2]oxazetidine	ketene+vinylimine

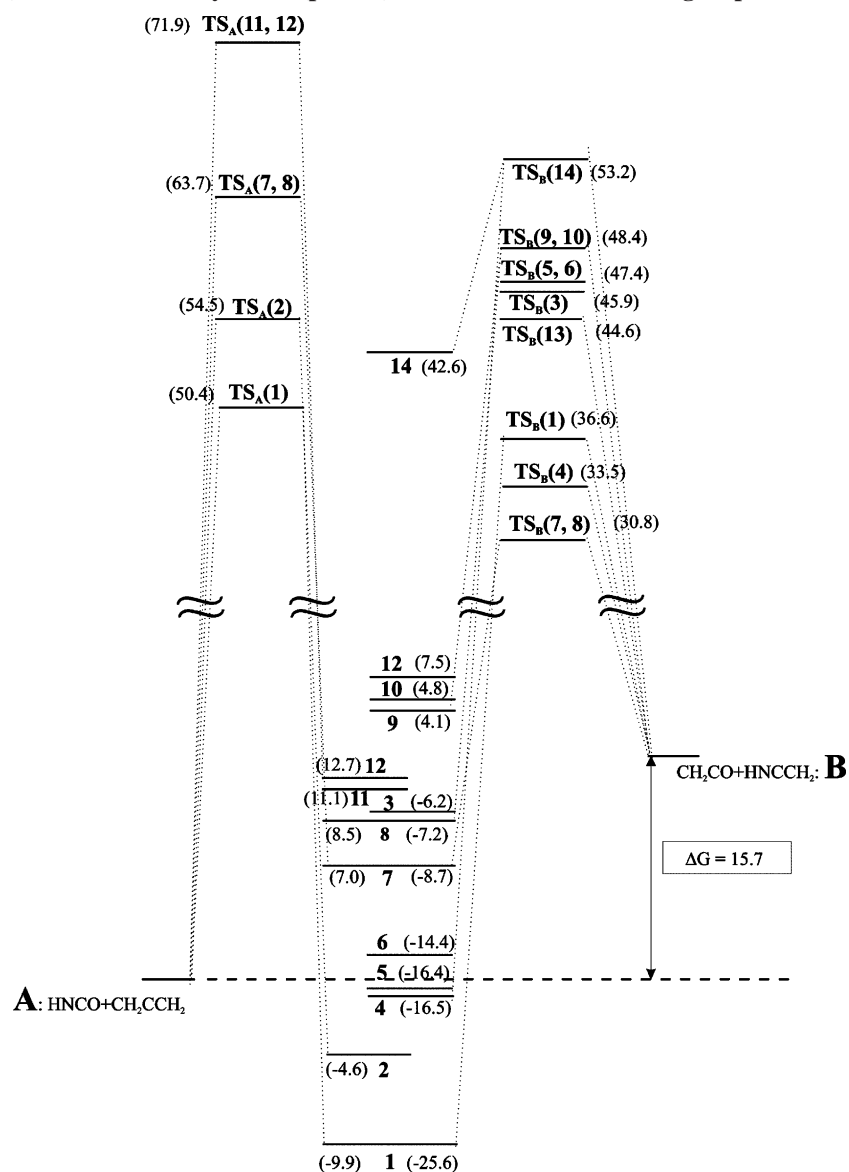
**SCHEME 1. Possible Product Structures Obtained from the [2 + 2] Cycloaddition of the Cumulenes Considered**

All the calculations were performed with the Gaussian98<sup>45</sup> and Gaussian03<sup>46</sup> software packages. The imaginary vibrations

were visualized by using the Molekel 4.0 program.<sup>47</sup> The bond critical points (BCPs) (3,−1) and the ring critical points (RCPs) (3,+1) in the TS structures were localized by using the AIM2000 program.<sup>48</sup>

## Results and Discussion

The [2 + 2] cycloadditions of allene with isocyanic acid (path A) and ketene with vinylimine (path B) can potentially lead to 6 and 11 products, respectively (Scheme 1, Table 1).

**CHART 1. Energetics in the Gas Phase,  $\Delta G$  ( $p = 1$  atm,  $T = 298$  K), of the [2 + 2] Cycloaddition Reaction of Allene–Isocyanic Acid (path A) and Ketene–Vinylimine (path B) Calculated at the MP2/aug-cc-pVDZ Level**

However, some products differ from each other only in a syn–anti configuration of the imine H-atom. Therefore, the number of TS structures is smaller, because the same TS can lead to a syn or anti isomer. This is the case for the following pairs of isomers: **5** and **6**, **7** and **8**, **9** and **10**, and **11** and **12**.

For the gas phase, selected geometrical parameters of the TSs are presented in Figures 2 and 3. The Gibbs free energy differences,  $\Delta G$ , defining the reaction energies and the activation barriers at 298 K, for the two types of the reaction paths are presented in Chart 1. Furthermore, the values from Chart 1, as well as the total energy differences corrected for the zero-point energies,  $\Delta E_{\text{ZPE}}$ , and interpretation of imaginary frequency modes of the TSs, are collected in Tables 2 and 3. The HOMO–LUMO orbital energy gaps for the reactants studied are gathered in Table 4.

For the lowest-energy pathways of both reactions, different solvent environments were included. The selected geometrical parameters for the TS structures and intermediates in solution are presented in Figure 5. For the lowest-energy pathways, the mechanisms in the gas phase and in solvents were confirmed by IRC calculations (Figures 1 and 4). The BCPs and RCPs are presented in Figures 6 and 7. Additionally, the geometric

**TABLE 2: MP2/Aug-cc-pVDZ Relative Reaction Energies with Respect to the Isolated Reactants (kcal/mol) for the [2 + 2] cycloaddition of allene to isocyanic acid in the gas phase**

	$\Delta E_{\text{ZPE}}$ , $\Delta E_a^a$	$\Delta G$ , $\Delta G_a^b$	frequency	mode interpretation <sup>c</sup>
path A: allene + isocyanic acid				
<b>1</b>	-21.48	-9.89		
TS <sub>A</sub> ( <b>1</b> )	39.84	50.35	730i	$\nu(\text{N1C4}) + \nu(\text{C2C3})$
<b>2</b>	-15.77	-4.61		
TS <sub>A</sub> ( <b>2</b> )	43.67	54.50	759i	$\nu(\text{N1C4}) + \nu(\text{C2C3})$
<b>7</b>	-4.64	6.97		
<b>8</b>	-3.15	8.48		
TS <sub>A</sub> ( <b>7,8</b> )	52.56	63.74	769i	$\nu(\text{O1C4}) + \nu(\text{C2C3})$
<b>11</b>	-0.42	11.14		
<b>12</b>	1.18	12.73		
TS <sub>A</sub> ( <b>11,12</b> )	61.34	71.85	1053i	$\nu(\text{O1C4}) + \nu(\text{C2C3})$

<sup>a</sup>  $\Delta E_{\text{ZPE}}$  stands for energies corrected for ZPE and  $\Delta E_a$  for activation barriers. <sup>b</sup>  $\Delta G$  stands for the Gibbs reaction energies and  $\Delta G_a$  for free Gibbs activation barriers. <sup>c</sup> The modes corresponding to the imaginary frequencies ( $\text{cm}^{-1}$ ) of the TS structures are interpreted in terms of internal motions.

details and energetics of the products, intermediates, and TSs studied are collected in Tables S1–S4 of the Supporting

**TABLE 3: MP2/Aug-cc-pVDZ Relative Reaction Energies with Respect to the Isolated Reactants (kcal/mol) for the [2 + 2] cycloaddition of ketene to vinylimine in the gas phase<sup>a</sup>**

	$\Delta E_{\text{ZPE}}$ , $\Delta E_a$	$\Delta G$ , $\Delta G_a$	frequency	mode interpretation
path B: ketene + vinylimine				
<b>1</b>	-37.37	-25.57		
TS <sub>B</sub> (2)	25.96	36.56	513i	$\nu(\text{C3C4})$
<b>3</b>	-17.96	-6.24		
TS <sub>B</sub> (3)	34.31	45.86	308i	$\nu(\text{N1C4})$
<b>4</b>	-27.58	-16.54		
TS <sub>B</sub> (4)	22.18	33.54	424i	$\nu(\text{C2C3})$
<b>5</b>	-27.60	-16.36		
<b>6</b>	-25.56	-14.43		
TS <sub>B</sub> (5,6)	35.88	47.39	286i	$\nu(\text{C1C4}) + \tau(\text{CH}_2)_{\text{vin}} + \tau(\text{CH}_2)_{\text{ket}}$
<b>7</b>	-20.53	-8.71		
<b>8</b>	-19.04	-7.21		
TS <sub>B</sub> (7,8)	19.65	30.82	248i	$\nu(\text{O1C4})$
<b>9</b>	-7.61	4.11		
<b>10</b>	-6.92	4.82		
TS <sub>B</sub> (9,10)	36.81	48.36	184i	$\tau(\text{CH}_2)$
<b>13</b>	-4.42	7.49		
TS <sub>B</sub> (13)	32.90	44.57	500i	$\nu(\text{O1C4}) + \tau(\text{CH}_2)_{\text{vin}}$
<b>14</b>	30.86	42.58		
TS <sub>B</sub> (14)	41.85	53.18	497i	$\gamma(\text{NH})$

<sup>a</sup> For abbreviations, see Table 2.

**TABLE 4: MP2/Aug-cc-pVDZ HOMO–LUMO Orbital Energy Gaps  $\Delta\epsilon$  between Reacting Systems**

interacting orbitals	$\Delta\epsilon$	
	kcal/mol	eV
HOMO (isocyanic acid)–LUMO (allene)	-307.699	-13.34
HOMO (allene)–LUMO (isocyanic acid)	-253.953	-11.01
HOMO (ketene)–LUMO (vinylimine)	-250.671	-10.87
HOMO (vinylimine)–LUMO (ketene)	-245.199	-10.63

Information (SI). For the lowest-energy TSs in the gas phase and water, atomic charges are presented in Figure S1 of the SI.

**Gas Phase. Energetics.** Two factors are important in determining the stability of a molecule: the stabilizing energy resulting from the formation of bonds between the atoms (the enthalpy term) and the destabilizing energy due to the loss of freedom involved in constraining the atoms within the molecular structure (the entropy term). The thermodynamic function which embraces both of these factors is the free energy—the fundamental quantity which controls the feasibility and the rates of all reactions. Therefore, below, we refer to the  $\Delta G$  values only. It is important, however, that for all studied reactions the entropy term ( $T\Delta S$ ) is quite constant (it varies within 2 kcal/mol, Tables S1 and S2). Thus, for the reaction studied practically, the enthalpy term differentiates the  $\Delta G$  values. Also, one can find  $\Delta E_{\text{ZPE}}$  values in Tables 2 and 3 and S1 and S2.

For the allene–isocyanic acid [2 + 2] cycloaddition reaction, there are no experimental values for either reaction energies or activation barriers. On the other hand, such a reaction was the subject of theoretical investigation; however, only the compounds endowed with the  $\beta$ -lactam ring structure, **1** and **2** (4- and 3-methylene-2-azetidinone), were considered at different levels of theory.<sup>23,24</sup> In this paper, we consider reactions leading to all possible four-membered ring products.

The reactions following path A toward **1** and **2** are exoergic, whereas those leading to the other possible products, 4- and 3-methylene-2-iminoxetanes, **7** and **8** and **11** and **12**, are endoergic (Chart 1, Table 2).

Also, the barrier heights toward the  $\beta$ -lactam molecules are lower than those toward 2-iminoxetanes, however, the reaction barriers of TS<sub>A</sub>(1) and TS<sub>A</sub>(2) (50 and 55 kcal/mol, respectively)

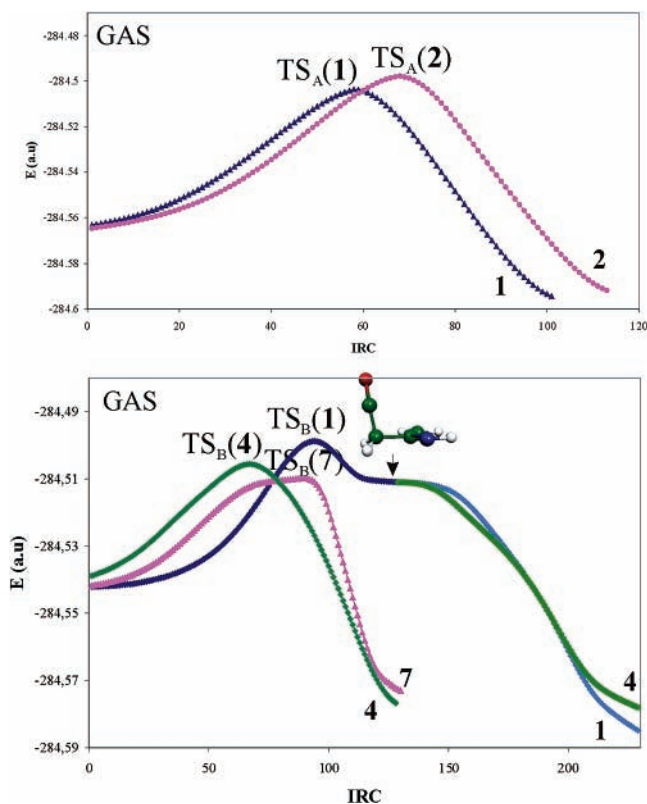


**Figure 1.** Gas-phase IRC profiles for the allene–isocyanic acid and ketene–vinylimine [2 + 2] cycloadditions. The molecular scheme corresponds to the bifurcation point.

are quite high to be overcome in spontaneous reactions. The barriers obtained by Cossio et al.<sup>24</sup> at the MP2/6-31+G\* level are close to our  $\Delta E_a$  values, namely, 39.7 and 43.6 kcal/mol<sup>24</sup> vs 39.9 and 43.7 kcal/mol for TS<sub>A</sub>(1) and TS<sub>A</sub>(2) in this paper, respectively. The reaction energies expressed in terms of  $\Delta E_{\text{ZPE}}$  do not agree so well.

In comparison with the allene–isocyanic acid reaction, the ketene–vinylimine cycloadditions run through lower activation barriers, and if they lead to the same product as in the path A, then they are much lower (Chart 1, Tables 3 and S2). They range from ca. 30 to 55 kcal/mol. The products are more stabilized as well.

However, in the reaction path B toward product **1**, thermodynamically the most stable, the activation barrier is not the lowest. It is higher than the TS<sub>B</sub>(7,8) by ca. 6 kcal/mol, and it can be stated that 2-iminoxetanes can possibly be formed owing to kinetic control. The 2-iminoxetane compounds are the main products in the vinylimine–aldehyde or ketene cycloadditions.<sup>30,34</sup> The least stable product of the reaction is 3,4-dimethylene-[1,2]oxazetidine, **14**, with both heteroatoms built into the ring and the barrier toward reactants equal to ca. 10 kcal/mol only. Thus, it is likely that **14** decomposes rapidly.

It is interesting to see why the activation barriers are lower in the ketene–vinylimine reaction than those in the allene–isocyanic acid one. The answer can be derived simply from an argument based on the frontier orbitals approximation (FOA).<sup>49</sup> According to the approximation, the stabilization effect is due to the (highest occupied molecular orbital–lowest unoccupied molecular orbital) HOMO–LUMO reactant orbitals interaction which is proportional to the overlap integral  $S$  and to  $1/\Delta\epsilon$ , where  $\Delta\epsilon = \epsilon_D^{\text{HOMO}} - \epsilon_A^{\text{LUMO}}$  is the energy separation between the two orbitals of the donor D and acceptor A molecules.<sup>50</sup> In the ketene–vinylimine cycloaddition, the HOMO–LUMO

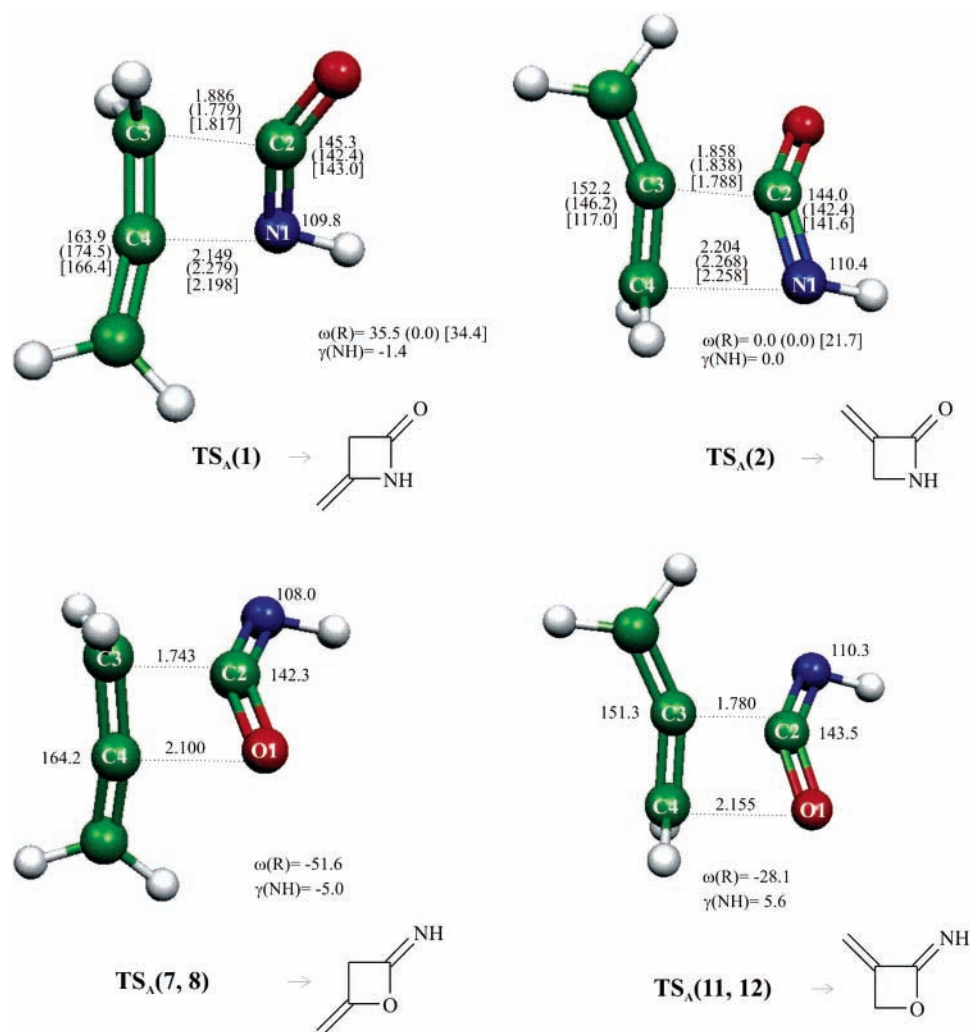


**Figure 2.** Atom numbering and selected geometrical parameters (angstroms and degrees) of the transition-state structures for the allene–isocyanic acid cycloaddition (path A) in the gas phase calculated at the MP2/aug-cc-pVDZ level. Parentheses and brackets include the HF/6-31G\* and MP2/6-31+G\* values,<sup>24</sup> respectively.

energy separation is smaller than that in the allene–isocyanic one (Table 4). Thus, the activation barriers in the former reaction are expected to be lower than those in the latter one.

For both reactions, for the lowest-energy pathways leading to **1** and **2** (in the allene–isocyanic acid reaction) and **1**, **4**, and **7** (in the ketene–vinylimine reaction), the IRC calculations were performed (Figure 1).

The IRC calculations have confirmed that the reactions are concerted. The only problem appeared in the IRC calculations leading to  $\beta$ -lactam **1** in the ketene–vinylimine reaction: the IRC calculations always stopped at a perpendicular arrangement of the components with one small imaginary frequency suggesting a rotation around the C2–C3 bond. This is probably a bifurcation point (Figure 1): rotation in one direction leads to **1** and in the other to **4**. The IRC calculations from that point performed for one reaction direction converged to **1** whereas for the other direction converged to **4**. Thus, the bifurcation point is a TS from the isomerization reaction between **1** and **4**.

**TS Geometries.** The selected geometrical parameters of the four TS structures toward the allene–isocyanic acid cycloaddition products are presented in Figure 2. More geometrical parameters can be found in Table S3. The geometrical parameters calculated at the HF/6-31G\* and MP2/6-31+G\* levels by Cossio et al.<sup>24</sup> are shown in parentheses and brackets, respectively (Figure 2). The  $\omega(R)$  angle reflects the deformation of

the four-membered ring and is defined as the dihedral angle of the 1–2–3–4 ring atoms. The  $\gamma(\text{NH})$  dihedral angle defines the position of the NH group hydrogen atom and is defined as the dihedral angle  $\gamma(\text{H}, \text{N}, \text{C}, \text{O})$  in  $\text{H}-\text{N}=\text{C}=\text{O}$  or  $\gamma(\text{H}, \text{N}, \text{C}, \text{C})$  in  $\text{H}-\text{N}=\text{C}=\text{CH}_2$  in the allene–isocyanic acid and ketene–vinylimine reactions, respectively. In products, it reflects the distortion of the H(N) atom from the four-membered ring plane.

Inspection into the geometrical parameters for the TSs of allene–isocyanic acid reactions indicates that the first-order saddle points of the  $\beta$ -lactam skeleton, TS<sub>A</sub>(1) and TS<sub>A</sub>(2), have  $C_1$  and the  $C_s$  symmetry, respectively (Figure 2). The TS geometries are in line with those of the previous calculations performed by Cossio et al.<sup>24</sup> for 4-methylene-2-azetidinone at the MP2/6-31+G\* level (Figure 2). However, for 3-methylene-2-azetidinone, there are two main differences: First, in our calculations, the allene angle is equal to 152°, whereas Cossio's angle is 117°. Second, the TS obtained here is planar, whereas Cossio's TS is skewed by 22°. On the other hand, planarity of the ring in the 3-methylene compounds is not observed to occur in TS<sub>A</sub>(11,12) and the ring deformation is significant in TS<sub>A</sub>(7,8). In 2-iminooxetane TSs, the intermolecular distances are slightly shorter than those for the  $\beta$ -lactam TS structures.

The eight TS structures considered in the ketene–vinylidene [2 + 2] cycloaddition lead to 11 possible four-membered ring products (Figure 3). Four of the TS structures are nearly planar.

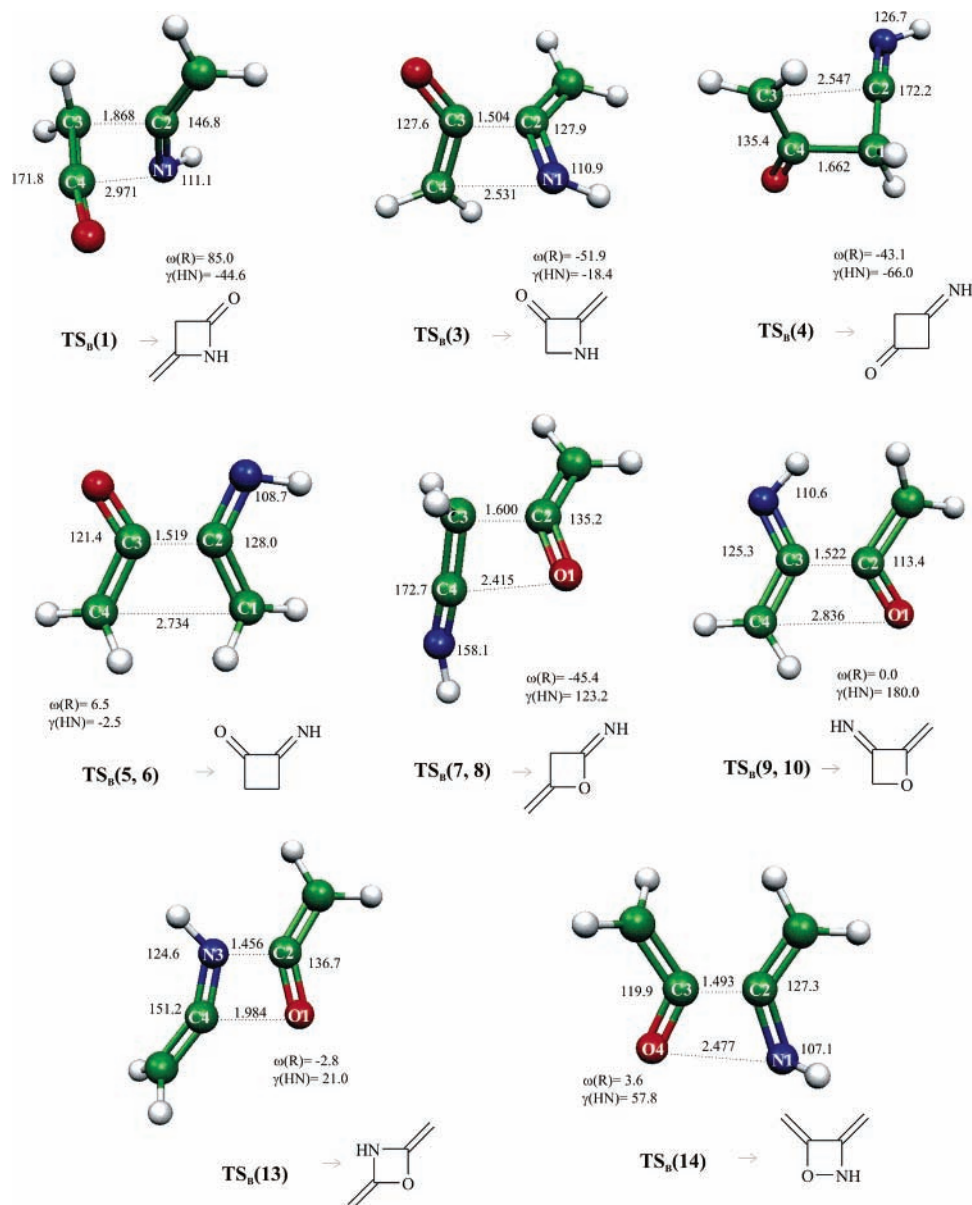


**Figure 3.** Atom numbering and selected geometrical parameters (angstroms and degrees) of the transition-state structures for the ketene-vinylimine cycloaddition (path B) calculated in the gas phase at the MP2/aug-cc-pVDZ level.

In three cases, TS<sub>B</sub>(1), TS<sub>B</sub>(4), and TS<sub>B</sub>(7,8), the angle of one of the components is almost unchanged and equal to ca. 170°. Probably, this small deformation of the angle is the reason the activation barriers are relatively low. For each TS structure, one of the newly forming bonds is much shorter than the other. Moreover, excluding TS<sub>B</sub>(1), TS<sub>B</sub>(4), and TS<sub>B</sub>(7,8), one of the bonds is already formed, as the differences between the distance in TS and the appropriate product do not exceed 0.05 Å (Table S4). Therefore, the reactions are highly asynchronous. In TS<sub>B</sub>(1), TS<sub>B</sub>(4), and TS<sub>B</sub>(7,8), the newly forming C-C bonds are much shorter than the N1-C4, C2-C3, and O1-C4 distances, respectively, yet much longer than those in the appropriate product. In TS<sub>B</sub>(13), the C2-N3 bond is formed earlier than the C4-O1 bond.

**Solvent Effect. Energetics.** Polar solvents have been shown to significantly stabilize zwitterionic complexes, consequently changing the topology of the free energy surface from the one-step in the gas phase to the two-step process.<sup>29</sup> Therefore, for the lowest-energy pathways (leading to products **1** and **2** in the allene-isocyanic acid reaction and to **1**, **4**, and **7** in the ketene-vinylimine reaction), solvent environments of different dielectric

constants (toluene, THF, acetonitrile, and water) have been simulated by the IEF-PCM method.<sup>43,51</sup> The energetics, lowest frequency motions, and mode interpretations obtained for the lowest-energy pathways in different solvents are collected in Table 5. In Table 6, the  $\Delta G$  values for different environments are juxtaposed to illustrate the tendencies produced by solvent effect.

As in the gas phase, the allene-isocyanic acid reactions in solvents are concerted (Figure 4), yet they run through slightly higher activation barriers and end up in products a bit more stabilized (Table 6).

The IRC calculations convince us that, in solvents, the ketene-vinylimine reactions leading to **4** and **7** become stepwise processes. The reaction leading to **1** in water and acetonitrile is a multistep process as well, however, in the other solvents, the second TS<sub>B</sub>2(**1**)<sub>s</sub> was not found: in toluene and THF, the supposed TS<sub>B</sub>2(**1**)<sub>s</sub> structure converged to TS<sub>B</sub>2<sup>-1</sup>(**4**)<sub>s</sub>. This suggests that this reaction is a one-step process in toluene and THF, yet convergence problems in obtaining the appropriate TSs in these solvents cannot be excluded entirely. For water and acetonitrile, when starting the IRC routine from the

**TABLE 5: MP2/Aug-cc-pVDZ Relative Reaction Energies with Respect to the Isolated Reactants (kcal/mol) Calculated in Different Solvents for the Two Lowest-Energy Pathways for the Allene–Isocyanic Acid and Ketene–Vinylimine [2 + 2] Cycloadditions<sup>a</sup>**

	$\Delta E_{\text{ZPE}}, \Delta E_a$	$\Delta G, \Delta G_a$	frequency	mode	interpretation
path A: allene + isocyanic acid in toluene ( $\epsilon = 2.379$ )					
<b>1<sub>s</sub></b>	-21.99	-10.72			
TS <sub>A</sub> ( <b>1</b> ) <sub>s</sub>	40.21	50.94	665i	$\nu(\text{N1C4}) + \nu(\text{C2C3})$	
<b>2<sub>s</sub></b>	-16.49	-5.49			
TS <sub>A</sub> ( <b>2</b> ) <sub>s</sub>	44.95	55.53	772i	$\nu(\text{N1C4}) + \nu(\text{C2C3})$	
path B: ketene + vinylimine in toluene ( $\epsilon = 2.379$ )					
<b>1<sub>s</sub></b>	-38.10	-26.62			
TS <sub>B</sub> 1( <b>1</b> ) <sub>s</sub>	25.41	35.80	539i	$\nu(\text{C2C3})$	
INT <sub>1s</sub>	<i>b</i>	<i>b</i>			
TS <sub>B</sub> 2( <b>1</b> ) <sub>s</sub>	<i>c</i>	<i>c</i>			
<b>7<sub>s</sub></b>	-20.28	-8.81			
TS <sub>B</sub> 1( <b>7</b> ) <sub>s</sub>	12.11	22.47	357i	$\nu(\text{C2C3})$	
INT <sub>7s</sub>	10.51	20.97			
TS <sub>B</sub> 2( <b>7</b> ) <sub>s</sub>	10.80	21.57	269i	$\nu(\text{O1C4})$	
<b>4<sub>s</sub></b>	-28.03	-17.12			
TS <sub>B</sub> 2 <sup>-1</sup> ( <b>4</b> ) <sub>s</sub>	18.39	29.64	128i	$\nu(\text{C1C4})$	
TS <sub>B</sub> 2 <sup>-7</sup> ( <b>4</b> ) <sub>s</sub>	17.71	28.72	463i	$\nu(\text{C2C3})$	
path A: allene + isocyanic acid in THF ( $\epsilon = 7.58$ )					
<b>1<sub>s</sub></b>	-22.36	-11.03			
TS <sub>A</sub> ( <b>1</b> ) <sub>s</sub>	40.10	50.98	600i	$\nu(\text{N1C4}) + \nu(\text{C2C3})$	
<b>2<sub>s</sub></b>	-17.09	-6.01			
TS <sub>A</sub> ( <b>2</b> ) <sub>s</sub>	45.95	56.57	777i	$\nu(\text{N1C4}) + \nu(\text{C2C3})$	
path B: ketene + vinylimine in THF ( $\epsilon = 7.58$ )					
<b>1<sub>s</sub></b>	-38.68	-27.14			
TS <sub>B</sub> 1( <b>1</b> ) <sub>s</sub>	24.94	35.39	564i	$\nu(\text{C2C3})$	
INT <sub>1s</sub>	<i>b</i>	<i>b</i>			
TS <sub>B</sub> 2( <b>1</b> ) <sub>s</sub>	<i>c</i>	<i>c</i>			
<b>7<sub>s</sub></b>	-19.95	-8.44			
TS <sub>B</sub> 1( <b>7</b> ) <sub>s</sub>	9.19	19.48	394i	$\nu(\text{C2C3})$	
INT <sub>7s</sub>	1.31	11.66			
TS <sub>B</sub> 2( <b>7</b> ) <sub>s</sub>	4.05	14.76	345i	$\nu(\text{O1C4})$	
<b>4<sub>s</sub></b>	-28.36	-17.39			
TS <sub>B</sub> 2 <sup>-1</sup> ( <b>4</b> ) <sub>s</sub>	16.66	27.88	234i	$\nu(\text{C1C4})$	
TS <sub>B</sub> 2 <sup>-7</sup> ( <b>4</b> ) <sub>s</sub>	13.59	24.65	551i	$\nu(\text{C2C3})$	
path A: allene + isocyanic acid in acetonitrile ( $\epsilon = 36.64$ )					
<b>1<sub>s</sub></b>	-22.54	-11.18			
TS <sub>A</sub> ( <b>1</b> ) <sub>s</sub>	39.94	50.87	567i	$\nu(\text{N1C4}) + \nu(\text{C2C3})$	
<b>2<sub>s</sub></b>	-17.38	-6.27			
TS <sub>A</sub> ( <b>2</b> ) <sub>s</sub>	46.41	57.03	778i	$\nu(\text{N1C4}) + \nu(\text{C2C3})$	
path B: ketene + vinylimine in acetonitrile ( $\epsilon = 36.64$ )					
<b>1<sub>s</sub></b>	-38.96	-27.40			
TS <sub>B</sub> 1( <b>1</b> ) <sub>s</sub>	24.55	35.01	577i	$\nu(\text{C2C3})$	
INT <sub>1s</sub>	<i>b</i>	<i>b</i>			
TS <sub>B</sub> 2( <b>1</b> ) <sub>s</sub>	13.40	24.40	225i	$\nu(\text{N1C4})$	
<b>7<sub>s</sub></b>	-19.77	-8.24			
TS <sub>B</sub> 1( <b>7</b> ) <sub>s</sub>	8.12	18.35	413i	$\nu(\text{C2C3})$	
INT <sub>7s</sub>	-2.93	7.46			
TS <sub>B</sub> 2( <b>7</b> ) <sub>s</sub>	1.18	11.92	383i	$\nu(\text{O1C4})$	
<b>4<sub>s</sub></b>	-28.53	-17.55			
TS <sub>B</sub> 2 <sup>-1</sup> ( <b>4</b> ) <sub>s</sub>	15.75	26.96	302i	$\nu(\text{C1C4})$	
TS <sub>B</sub> 2 <sup>-7</sup> ( <b>4</b> ) <sub>s</sub>	11.60	22.69	584i	$\nu(\text{C2C3})$	
path A: allene + isocyanic acid in water ( $\epsilon = 78.39$ )					
<b>1<sub>s</sub></b>	-22.55	-10.78			
TS <sub>A</sub> ( <b>1</b> ) <sub>s</sub>	39.86	51.22	561i	$\nu(\text{N1C4}) + \nu(\text{C2C3})$	
<b>2<sub>s</sub></b>	-17.44	-5.91			
TS <sub>A</sub> ( <b>2</b> ) <sub>s</sub>	46.47	57.52	778i	$\nu(\text{N1C4}) + \nu(\text{C2C3})$	
path B: ketene + vinylimine in water ( $\epsilon = 78.39$ )					
<b>1<sub>s</sub></b>	-38.99	-27.43			
TS <sub>B</sub> 1( <b>1</b> ) <sub>s</sub>	24.45	34.92	580i	$\nu(\text{C2C3})$	
INT <sub>1s</sub>	14.76	25.49			
TS <sub>B</sub> 2( <b>1</b> ) <sub>s</sub>	13.15	24.16	203i	$\nu(\text{N1C4})$	
<b>7<sub>s</sub></b>	-19.74	-8.22			
TS <sub>B</sub> 1( <b>7</b> ) <sub>s</sub>	7.93	18.22	332i	$\nu(\text{C2C3})$	
INT <sub>7s</sub>	-3.77	6.54			
TS <sub>B</sub> 2( <b>7</b> ) <sub>s</sub>	-2.16	9.03	394i	$\nu(\text{O1C4})$	
<b>4<sub>s</sub></b>	-28.61	-17.58			
TS <sub>B</sub> 2 <sup>-1</sup> ( <b>4</b> ) <sub>s</sub>	15.46	26.68	316i	$\nu(\text{C1C4})$	
TS <sub>B</sub> 2 <sup>-7</sup> ( <b>4</b> ) <sub>s</sub>	11.24	22.34	589i	$\nu(\text{C2C3})$	

<sup>a</sup> For abbreviations, see Table 2. INT stands for an intermediate state between TS1 and TS2 (see Figure 4). <sup>b</sup> The INT<sub>1s</sub> structure converged to **1**. <sup>c</sup> The TS<sub>B</sub>2(**1**)<sub>s</sub> structure converged to TS<sub>B</sub>2<sup>-1</sup>(**4**).

**TABLE 6: MP2/Aug-cc-pVDZ Relative Reaction Energies with Respect to the Isolated Reactants (kcal/mol) Calculated in the Gas Phase and in Different Solvents for the Lowest-Energy Pathways for Allene–Isocyanic Acid and Ketene–Vinylimine [2 + 2] Cycloadditions<sup>a</sup>**

	gas	toluene	THF	acetonitrile	water
path A: allene + isocyanic acid					
<b>1<sub>s</sub></b>	-9.89	-10.72	-11.03	-11.18	-10.78
TS <sub>A</sub> ( <b>1</b> ) <sub>s</sub>	50.35	50.94	50.98	50.87	51.22
<b>2<sub>s</sub></b>	-4.61	-5.49	-6.01	-6.27	-5.91
TS <sub>A</sub> ( <b>2</b> ) <sub>s</sub>	54.50	55.53	56.57	57.03	57.52
path B: ketene + vinylimine					
<b>1<sub>s</sub></b>	-25.57	-26.62	-27.14	-27.40	-27.43
TS <sub>B</sub> 1( <b>1</b> ) <sub>s</sub>	36.56	35.80	35.39	35.01	34.92
INT <sub>1s</sub>		a	a	a	25.49
TS <sub>B</sub> 2( <b>1</b> ) <sub>s</sub>		b	b	24.40	24.16
<b>7<sub>s</sub></b>	-8.71	-8.81	-8.44	-8.24	-8.22
TS <sub>B</sub> 1( <b>7</b> ) <sub>s</sub>	30.82	22.47	19.48	18.35	18.22
INT <sub>7s</sub>		20.97	11.66	7.46	6.54
TS <sub>B</sub> 2( <b>7</b> ) <sub>s</sub>		21.57	14.76	11.92	9.03
<b>4<sub>s</sub></b>	-16.54	-17.12	-17.39	-17.55	-17.58
TS <sub>B</sub> <sup>-12</sup> ( <b>4</b> ) <sub>s</sub>	33.54	29.64	27.88	26.96	26.68
TS <sub>B</sub> <sup>-72</sup> ( <b>4</b> ) <sub>s</sub>		28.72	24.65	22.69	22.34

<sup>a</sup> INT stands for an intermediate state between TS1 and TS2 (see Figure 4). <sup>b</sup> Converged to the  $\beta$ -lactam product **1**. <sup>c</sup> Converged to TS<sub>B</sub><sup>-12</sup>(**4**).

TS<sub>B</sub>2(**1**)<sub>s</sub>, connecting intermediate and product, a problem appears. The IRC calculations fail at a point of energy much below the intermediate INT<sub>1s</sub> detected by another IRC scan started from TS<sub>B</sub>1(**1**)<sub>s</sub>. This may be interpreted in the following way: in water and in acetonitrile, between INT<sub>1s</sub> and TS<sub>B</sub>2(**1**)<sub>s</sub>, there is a third TS and a second intermediate, however, they remain undetected. The IRC routine failed at a bifurcation on path B toward **1**. We suppose that the bifurcation is just a critical point on the path either toward reactants or toward that new intermediate (Figure 4).

The reaction toward **4** is an interesting case. It is a stepwise process, however, there are two ways to reach **4**. One way proceeds from INT<sub>1s</sub>, whereas the second proceeds from INT<sub>7s</sub> (Figure 4). The appropriate TSs are denoted as TS<sub>B</sub>2<sup>-1</sup>(**4**)<sub>s</sub> and TS<sub>B</sub>2<sup>-7</sup>(**4**)<sub>s</sub>, respectively. There is no separate TS<sub>B</sub>1(**4**)<sub>s</sub> because it is identical with either TS<sub>B</sub>1(**1**)<sub>s</sub> or TS<sub>B</sub>1(**7**)<sub>s</sub> (Figure 4). Moreover, the intermediates INT<sub>1s</sub> and INT<sub>7s</sub> are also common to the two pathways.

As for the gas phase, the activation barriers toward **7** remain the lowest. The TS<sub>B</sub>1(**1**)<sub>s</sub> and TS<sub>B</sub>1(**7**)<sub>s</sub> barriers are lower than those for TS<sub>B</sub>(**1**) and TS<sub>B</sub>(**7**) and the larger the dielectric constant, the lower the barrier (Table 6). In water, the barriers are lowered by ca. 1.6 and 12.6 kcal/mol, respectively. For a similar ketene–imine reaction toward  $\beta$ -lactam, water was found to reduce the free energy of activation by 4.5 kcal/mol.<sup>29b</sup> Also, one can see the great influence of the solvent on the energy of INT<sub>7s</sub>: 21.0 kcal/mol in toluene, whereas the energy is 6.5 kcal/mol in water.

Only in water we did localize INT<sub>1s</sub>. In toluene, THF, and acetonitrile, optimization of the structure, where the IRC routine stopped, converged to **1**. Thus, the IRC routine suggests the existence of either an intermediate structure or a bifurcation point, whereas the optimization routine suggests the absence of such points. It is interesting that the geometry of INT<sub>1w</sub> found in water is very similar to that of the bifurcation point in the gas-phase reaction toward **1** (Figure 1).

**TS Geometries.** The selected geometrical parameters of the TS structures and intermediates which manifest themselves in the course of the allene–isocyanic acid and the ketene–vinylimine cycloaddition reactions in different solvents are presented in Figure 5 and Tables S3 and S4a.



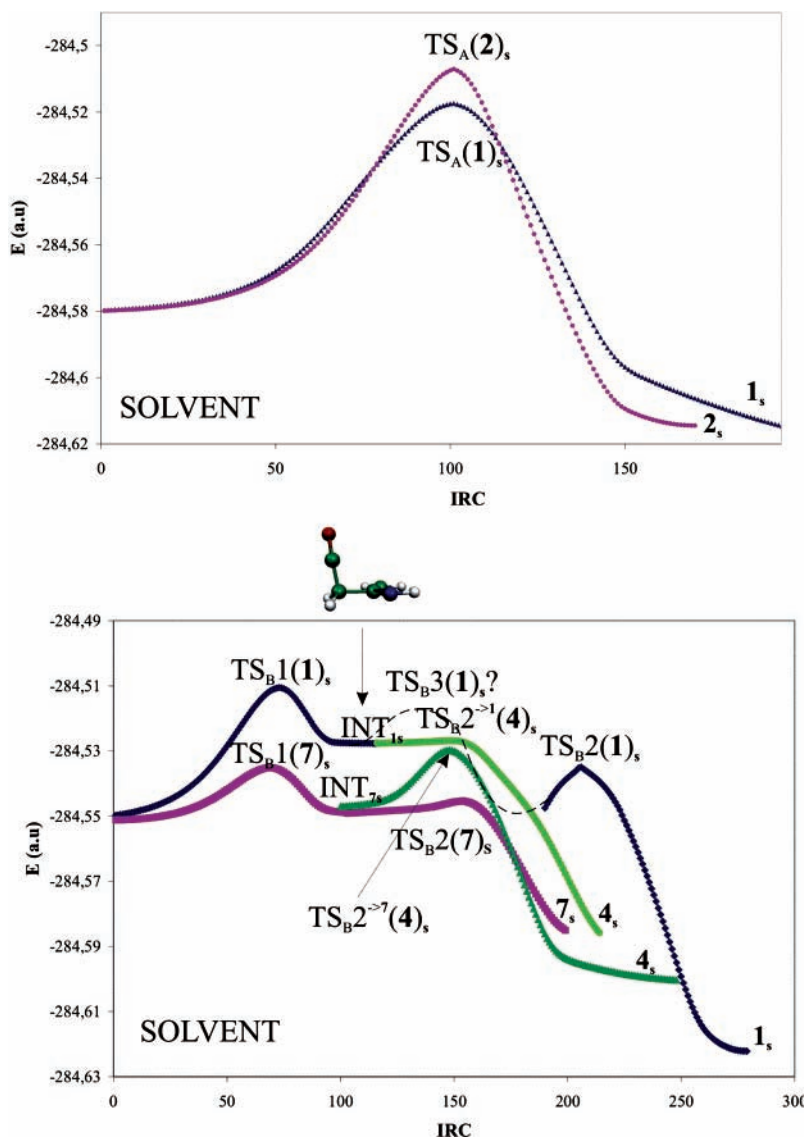


**Figure 4.** Schematic IRC profiles for the allene–isocyanic acid and ketene–vinylimine [2 + 2] cycloadditions in solvents. The supposed profiles are denoted by dashed lines.

In the case of the allene–isocyanic acid reaction, minor differences are found to occur between the geometrical parameters of TSs and the products in the gas and solvent phases (Table S3). The larger the dielectric constants, the longer the C=O and the N–H bond distances. This is connected with the solute–solvent interactions. In comparison to the gas phase, in solvent, the N1–C4 and C2–C3 distances in TSs are longer and shorter, respectively. Moreover, the  $TS_A(1)_s$  structure is more deformed: the ring deformation increases from  $35^\circ$  in gas to  $56^\circ$  in water.

In the case of the ketene–vinylimine reaction, the solvent shifts TS1 significantly toward the entrance channel as the reactants are more separated in both  $TS_B1(1)_s$  and  $TS_B1(7)_s$  (Figure 5, Table S4a). The larger the dielectric constant, the greater the interreactant distance. In solvents,  $TS1_B(7)_s$ , located between the intermediate  $INT_{7s}$  and reactants, is much more deformed than  $TS_B(7)$  found for the gas phase. The deformation angle  $\omega(R)$  is equal to  $-88^\circ$  in water, whereas it is  $-46^\circ$  in the gas phase. The  $INT_{7s}$  is similar to the  $TS_B(7)$  in gas, yet the ring is more deformed, by about  $10^\circ$ .

When compared to the gas phase, the solvent significantly shifts  $TS_B2(1)_s$ , located between the intermediate INT and product, toward the exit channel, as the C–C and C–N bond

distances decrease from 1.868 to 1.536 Å and from 2.971 to 2.354 Å, respectively. Similar results are obtained for  $TS_B2(7)_s$ : the larger the solvent dielectric constant, the shorter the C–C and C–O distances. With an increase in the dielectric constant, the  $TS_B2(7)_s$  becomes geometrically similar to the product: the four-membered ring becomes more and more planar, yet still in water the O1–C4 distance in TS is longer by ca. 1.2 Å than in product.

The  $TS_B2^{-7}(4)_s$  is similar to the  $TS_B(4)$  structure found in the gas phase, yet both intersystem distances are shorter in solvent than in a vacuum, and in solvents, the ring structure is less deformed than in the gas phase. On the other hand,  $TS_B2^{-1}(4)_s$  becomes similar to  $INT_{1s}$  in less polar solvents. The smaller the dielectric constant, the more deformed  $TS_B2^{-1}(4)_s$  becomes.

Finally, let us state that the presence of a solvent significantly increases the asynchronicity of the reactions. This will be also observed in the analysis of the reaction mechanisms.

**[2 + 2] Cycloaddition Mechanisms.** The early reaction mechanism concepts were based on the Woodward–Hoffmann (W–H) orbital symmetry conservation rules.<sup>52</sup> Since even ethene dimerization does not proceed according to the W–H rules,<sup>53</sup> they seem to be purely conceptual. Now, the cycloadd-

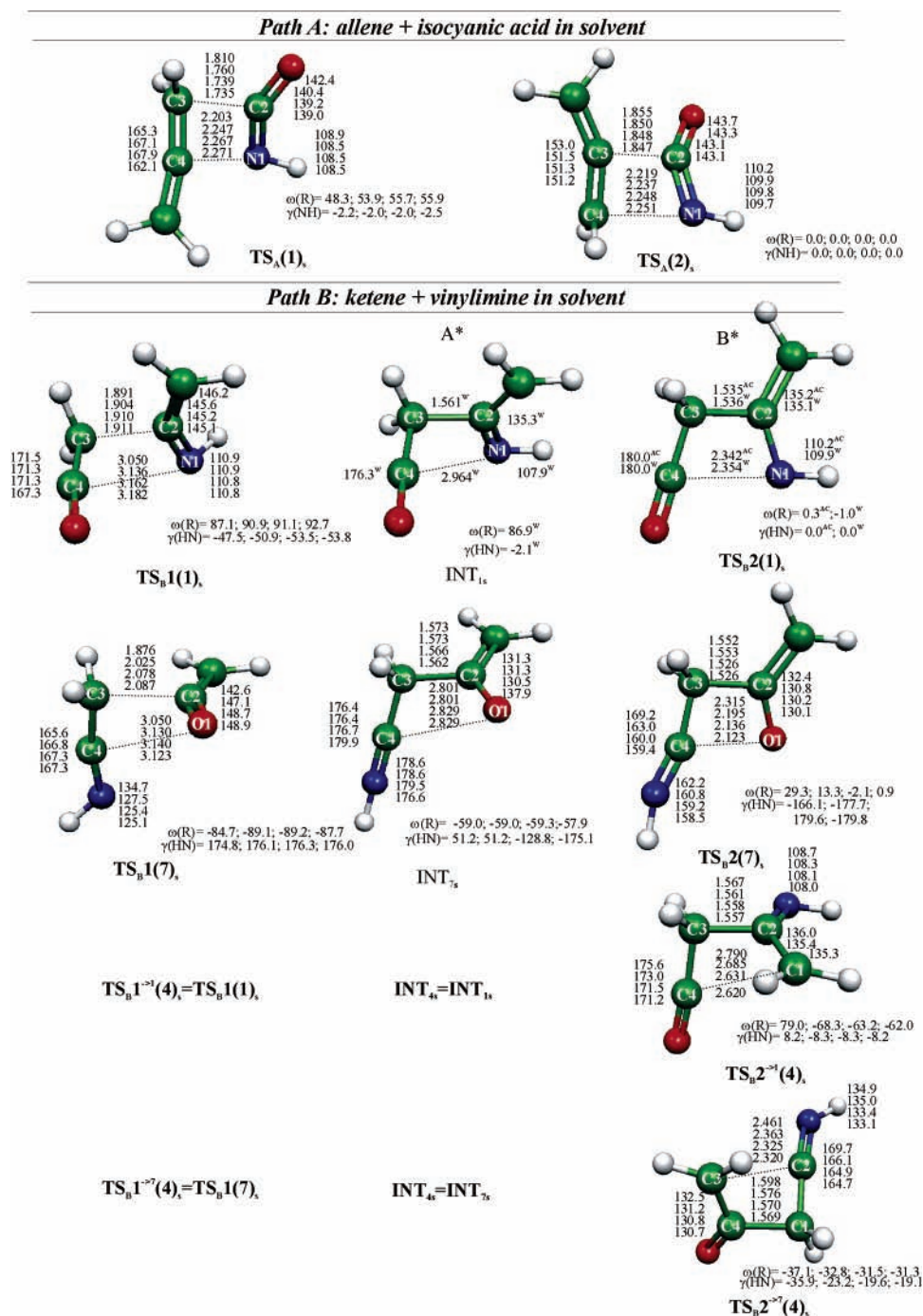


**Figure 5.** Atom numbering and selected geometrical parameters (angstroms and degrees) of the transition-state structures for the ketene–vinylimine cycloaddition (path B) calculated in different solvents (values from toluene, THF, acetonitrile, and water, respectively) at the MP2/aug-cc-pVDZ level. AC stands for acetonitrile and W for water.

dition reactions are analyzed in terms of pericyclic and pseudopericyclic types of reactions rather than the W–H rules.<sup>52</sup> The W–H rules were formulated only for pericyclic reactions. A pericyclic reaction is concerted and takes place on a closed curve, that is, it requires an orbital overlap around the ring of breaking and forming bonds.<sup>52</sup> The transition structures of pericyclic reactions are expected to be highly nonplanar. In some concerted reactions taking place on a cyclic curve, the orbital overlap does not occur on the whole ring.<sup>54–58</sup> As a consequence, disconnections in orbital overlap appear in the TS and the TS ring is close to planar. This type of reaction was called by Lemaire the pseudopericyclic type.<sup>59</sup> The pseudopericyclic reactions cannot be symmetry forbidden, they have planar geometry of the TS, and often have low activation barriers.<sup>54</sup>

Different theoretical approaches have been used to differentiate the pseudopericyclic from the pericyclic type: the natural bond analysis (NBO) of the TSs,<sup>54,55</sup> magnetic properties and aromaticity of the TSs,<sup>56,57</sup> anisotropy of the current induced density (ACID) analysis,<sup>55</sup> electron localization function (ELF),<sup>58</sup> and ellipticity of the electron density.<sup>60</sup>

Finally, if the reaction is not concerted, that is, it is multistep, it cannot be classified as pericyclic or pseudopericyclic.

It is known that, for nonpolar reagents, the [2 + 2] cycloaddition generally proceeds via a diradical intermediate; for polar reagents, the [2 + 2] cycloaddition proceeds generally stepwise via a zwitterionic intermediate.<sup>61</sup> For cumulenes, the [2 + 2] cycloadditions were originally thought to go by a stepwise mechanism; however, this picture had to be revised,

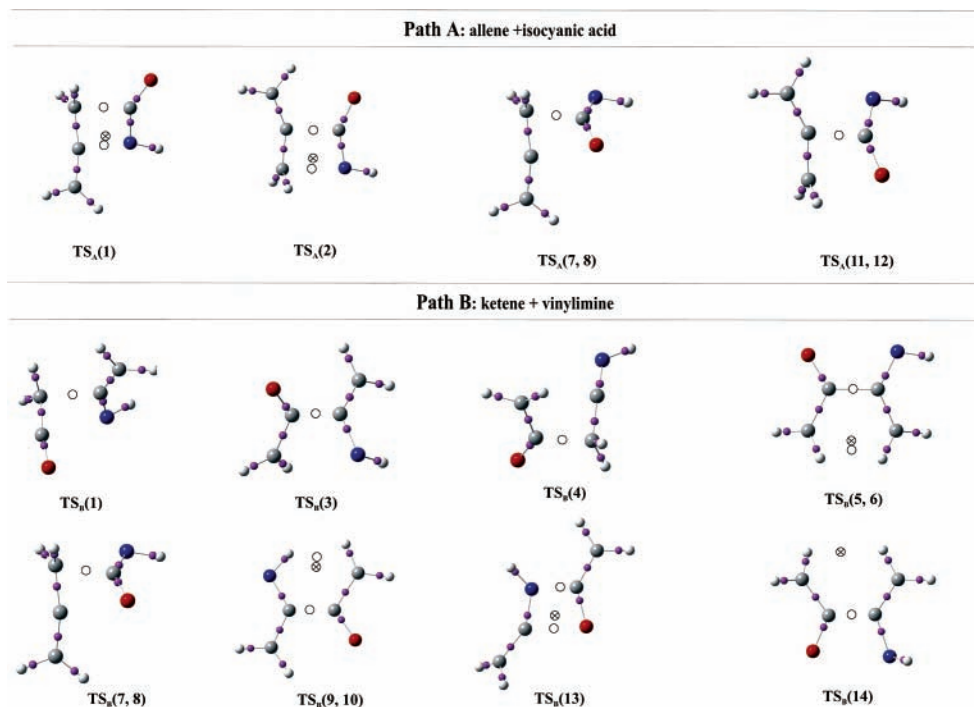


**Figure 6.** AIM analysis of the transition-state structures for allene–isocyanic acid (path A) and ketene–vinylimine (path B) reactions calculated at the MP2/aug-cc-pVDZ level for the gas phase. The bond critical points (3,−1) are shown either as small balls (ordinary bonds) or as open circles (newly formed bonds). The ring critical points (3,+1) are shown as crossed, open circles.

when the cycloadditions of ketenes to certain olefins were shown to be concerted.<sup>62</sup> In this paper, we consider the cycloadditions of polar cumulenes such as isocyanic acid, ketene, and vinylimine, therefore, we do not take into account the stepwise mechanism via any diradical intermediate.

For all the TSs studied, we performed the AIM analysis of the electron density and found all the BCPs (3,−1) and the RCP (3,+1). We assumed the presence of two new BCPs, between the atoms in a TS which had to be connected by a new  $\sigma$ -bond in the product, to indicate a pericyclic type of [2 + 2] cycloaddition, which was always additionally confirmed by the presence of the RCP. On the other hand, the presence of only one new BCP (always accompanied by the absence of an RCP) indicated the discontinuity of the orbital overlap in the newly formed ring and suggested the reaction to be a pseudopericyclic type. Another problem appears, however. Only some of the TSs are planar as needed for the reaction to be classified as pseudopericyclic.<sup>51b</sup> The reactions with TSs which are nonplanar and exhibit discontinuity can be classified as neither pericyclic nor ordinary pseudopericyclic. The latter type of the reaction is what we call here the nonplanar pseudopericyclic (NP-pseudopericyclic) reaction. Now, another (minor) problem arises: which TS ring nonplanarity is sufficient for the reaction to be classified as NP-pseudopericyclic. Some authors classified the reaction with TS nonplanarity of ca. 30° as pseudopericyclic.<sup>22</sup> Here, we arbitrarily accept the TS nonplanarity from −45° to +45° for the reaction to be classified as pseudopericyclic, and thus, NP-pseudopericyclic is the reaction with discontinuity and ring nonplanarity exceeding 45°. Last but not least, in two cases (namely, TS<sub>B</sub>(9,10) and TS<sub>B</sub>(14)), the new BCP and RCP indicate hydrogen-bond-like interaction<sup>63</sup> in the TS rather than  $\sigma$ -bond formation. Those critical points were ignored in the classification of the reaction mechanism.

Following the above argumentation, the allene–isocyanic acid gas-phase reactions toward  $\beta$ -lactams **1** and **2** are pericyclic. Each of the TS<sub>A</sub>(1) and TS<sub>A</sub>(2) exhibits two new BCPs and one RCP connected with cycle formation (Figure 6). On the other hand, the allene–isocyanic acid gas-phase reactions toward

iminoxetanes (**7**, **8**, **11**, and **12**) are pseudopericyclic, yet those toward **7** and **8** with substantially nonplanar TSs are NP-pseudopericyclic whereas those toward **11** and **12** are ordinary pseudopericyclic.

The solvent effect does not change the character of the IRC reaction profiles for path A reactions toward **1** and **2**, whereas the AIM analysis shows the mechanism of the reaction toward **1** to change from pericyclic in the gas phase to NP-pseudopericyclic in solvent (Figure 7). Modification of the environment does not affect the pericyclic mechanism of the reaction toward **2**.

The AIM analysis of the TSs in the ketene–vinylimine reactions in the gas phase (Figure 6) shows the most probable two reactions toward **1** and **7(8)** to be NP-pseudopericyclic. The same holds true for the reactions toward **3** whereas the reaction toward **4** is (ordinary) pseudopericyclic. On the other hand, the reactions toward **13** and **5(6)** are undoubtedly pericyclic. The reactions toward **9(10)** and **14** need more comments. In the TS<sub>B</sub>(9,10), two new BCPs and one RCP appear; however, one BCP and RCP are on the “wrong side” of the newly formed C2–C3 bond. Thus, their presence indicates an intramolecular H⋯H interaction rather than a new bond formation. On the “proper side”, that is, between O4 and C1, no BCP appears. Therefore, the reaction has to be classified as pseudopericyclic. A similar situation occurs for TS<sub>B</sub>(14): the additional RCP detected is placed between H-atoms, whereas between the N1–O4 atoms no critical point is present. Analogously, the reaction is pseudopericyclic.

The solvent medium considered for the most important reactions toward **7** and **4** changed the mechanism of the reactions from concerted to multistep. Therefore, they cannot be classified in terms of (pseudo)pericyclicity. However, if the reaction toward **1** is a one-step process (what cannot be excluded in the less polar solvents), then it should be considered as the NP-pseudopericyclic type of reaction (Figure 7).

Inspection into the atomic charges, calculated for the gas phase and for water as the most polar solvent, to check whether

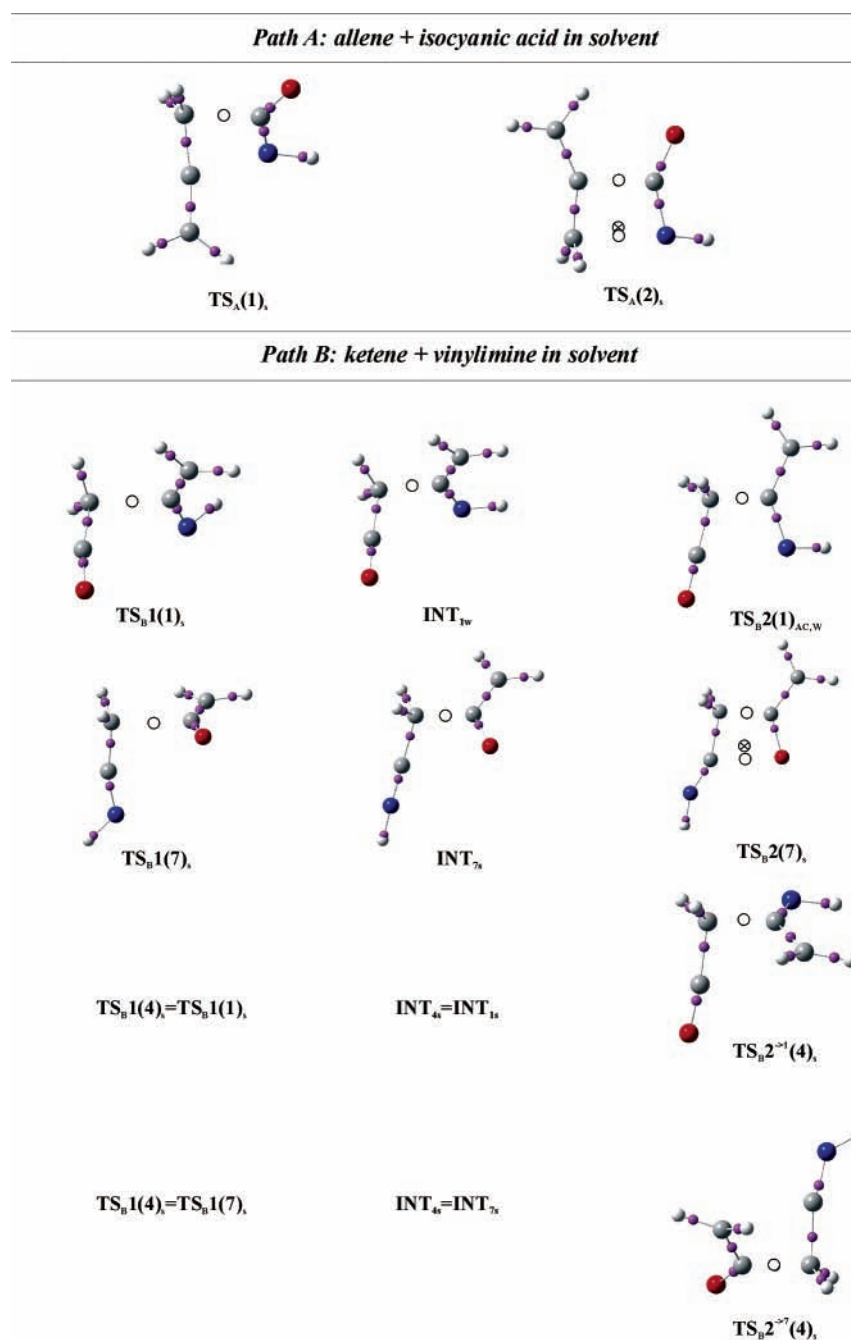


**Figure 7.** AIM analysis of the transition-state structures for the allene–isocyanic acid (path A) and ketene–vinylimine (path B) reactions in water calculated at the MP2/aug-cc-pVDZ level. The bond critical points (3,−1) are shown either as small balls (ordinary bonds) or as open circles (newly formed bonds). The ring critical points (3,+1) are shown as crossed, open circles.

the TSs studied possess a zwitterionic character or not, revealed a multicenter charge separation instead of a two-center one expected for a zwitterion (Figure S1). Moreover, the charge differences are often larger within one component than between the two components (Figure S1). Thus, a description of the reaction mechanisms in terms of zwitterionic charge separation seems to be oversimplified.

### Conclusions

The [2 + 2] cycloaddition reaction paths for allene–isocyanic acid (path A) and ketene–vinylimine (path B) additions were investigated at the MP2/aug-cc-pVDZ level. There are 14 possible four-membered products of these reactions and some of them can be formed along the two paths, thus altogether 17 reactions were taken into account. Some of the products differed

by only syn–anti isomerism at the imine group. Therefore, only 12 TSs were considered. In the gas phase, the reactions toward the  $\beta$ -lactam ring molecules of path A are exoergic, whereas those leading to 2-iminooxetanes are endoergic. The activation barriers in the allene–isocyanic acid reactions are fairly high, 50–70 kcal/mol, whereas those of the ketene–vinylimine cycloaddition fall into an interval of 30–55 kcal/mol. One can connect the barrier heights with the energy gaps between the HOMO and LUMO orbitals of the reactants. The gap is much lower for the ketene–vinylimine reaction than that for the allene–isocyanic acid one. Moreover, there are also geometrical arguments for the lower activation barriers: in the two TSs of the ketene–vinylimine reaction toward either 4-methylene-2-azetidinone, 3-imino-cyclobutanone, or 4-methylene-2-iminooxetane, deformation of one of the reaction partner molecules in

the TS is quite small. Although, in reaction path B, the 4-methylene-2-azetidinone compound is predicted to be the most stable thermodynamically, the reaction toward 4-methylene-2-iminoxetane exhibits an activation barrier lower by ca. 6 kcal/mol, and therefore, the latter compound seems to be obtainable owing to kinetic control. The TS geometries of path B indicate that one of the newly created bonds is almost formed. All the reactions studied for the gas phase were found to be concerted and asynchronous.

For the allene–isocyanic acid [2 + 2] cycloaddition, the reaction mechanism is concerted in both the gas phase and the solvent. Moreover, only small differences are found to occur in energetics and geometry between the studied structures in the gas phase and in the solvent. In contrast, the solvent changes the ketene–vinylimine reaction leading to **1**, **7**, and **4** from concerted to multistep processes. In comparison to the gas phase, significant lowering of activations barriers occurs when the solvent is included.

The AIM analysis of the electron density distribution in the TS structures allowed us to distinguish the pericyclic from pseudopericyclic and from the NP-pseudopericyclic types of reactions.

**Acknowledgment.** Grant No. G19-4 from the Interdisciplinary Center of Mathematical and Computer Modeling (ICM) of Warsaw University is gratefully acknowledged for a generous allotment of computer time. The work was financially supported by the ICRI (Warsaw) from the statutory activity.

**Supporting Information Available:** The MP2/aug-cc-pVDZ energies, for both the gas-phase and water mediums, energies corrected for ZPE, and the Gibbs free energies for all products, intermediates, and appropriate transition structures considered in this paper as well as the detailed MP2/aug-cc-pVDZ calculated geometries are collected in Tables S1–S4. The charges from electrostatic potentials using a grid-based method (ChelpG) are gathered in Figure S1. This material is available free of charge via the Internet at <http://pubs.acs.org>.

## References and Notes

- Fleming, A. On the Antibacterial Action of Cultures of a Penicillium, with Special Reference to Their Use in the Isolation of *B. influenzae*. *Br. J. Exp. Pathol.* **1929**, *10*, 226–236.
- Miller, M. J. Recent Aspects of the Chemistry of  $\beta$ -Lactams. *Tetrahedron* **2000**, *56*, preface.
- Alcaide, B.; Almendros, P. 4-Oxoazetidine-2-carbaldehydes as useful building blocks in stereocontrolled synthesis. *Chem. Soc. Rev.* **2001**, *30*, 226–240.
- Katzung, B. G. *Basic & Clinical Pharmacology*; McGraw-Hill Medical: New York, 2004.
- Slusarchyk, W. A.; Dejneka, T.; Gordon, E. M.; Weaver, E. R.; Koster, W. H. Monobactams: Ring Activity *N*-1-Substituents in Monocyclic  $\beta$ -Lactam Antibiotics. *Heterocycles* **1984**, *21*, 191.
- Imada, A.; Kitano, K.; Kintaka, K.; Muroi, M.; Asai, M. Sulfazecin and isosulfazecin, novel  $\beta$ -lactam antibiotics of bacterial origin. *Nature* **1981**, *289*, 590–592.
- Ogilvie, W. W.; Yoakim, C.; Do, F.; Hache, B.; Lagace, L.; Naud, J.; O'Meara, J. A.; Deziel, R. Synthesis and antiviral activity of monobactams inhibiting the human cytomegalovirus protease. *Bioorg. Med. Chem.* **1999**, *7*, 1521–1531.
- Adlington, R. M.; Baldwin, J. E.; Chen, B.; Cooper, S. L.; McCoull, W.; Pritchard, G. J.; Howe, T. J. Design and synthesis of novel monocyclic  $\beta$ -lactam inhibitors of prostate specific antigen. *Bioorg. Med. Chem. Lett.* **1999**, *7*, 1689–1694.
- Han, W. T.; Trehan, A. K.; Wright, J. J.; Federici, M. E.; Seiler, S. M.; Meanwell, N. A. Azetidin-2-one Derivatives as Inhibitors of Thrombin. *Bioorg. Med. Chem.* **1995**, *3*, 1123–1143.
- Doherty, J. B.; Ashe, B. M.; Barker, P. L.; Blacklock, T. J.; Butcher, J. W.; Chandler, G. O.; Dahlgren, M. E.; Davies, P.; Dorn, C. P.; Finke, P. E.; Firestone, R. A.; Hagman, W. K.; Halgren, T.; Knight, W. B.; Maycock, A. L.; Navia, M. A.; O'Grady, L.; Pisano, J. M.; Shah, S. K.; Thompson, K. R.; Weston; Zimmerman, M. Inhibition of human leukocyte elastase. Inhibition by C-7 substituted cephalosporin *tert*-butyl esters. *J. Med. Chem.* **1990**, *33*, 2513–2521.
- (a) Gómez-Gallego, M.; Mancheño, M. J.; Sierra, M. Non-Classical Polycyclic  $\beta$ -Lactams. *Tetrahedron* **2000**, *56*, 5743–5774. (b) Cirilli, R.; Del Giudice, M. R.; Ferretti, R.; La Torre, F. Conformational and temperature effects on separation of stereoisomers of C3, C4-substituted  $\beta$ -lactamic cholesterol absorption inhibitor on amylose-based chiral stationary phases. *J. Chromatogr. A* **2001**, *923*, 27–36. (c) Burnett, D. A.; Caplen, M. A.; Domalski, M. S.; Browne, M. E.; Davis, H. R.; Clader, J. W. Synthesis of Iodinated Biochemical Tools Related to the 2-Azetidinone Class of Cholesterol Absorption Inhibitors. *Bioorg. Med. Chem. Lett.* **2002**, *12*, 311–314.
- (a) Kingston, D. I. Taxol, a molecule for all seasons. *Chem. Commun.* **2001**, 867–880. (b) Hodous, B. L.; Fu, G. C. Enantioselective Staudinger Synthesis of  $\beta$ -lactams Catalyzed by a Planar-Chiral Nucleophile. *J. Am. Chem. Soc.* **2002**, *124*, 1578–1579. (c) Palomo, C.; Arrieta, A.; Cossio, F. P.; Aizpurua, J. M.; Mielgo, A.; Aurrekoetxea, N. Highly Stereoselective Synthesis of  $\alpha$ -Hydroxy  $\beta$ -Amino acids through  $\beta$ -Lactams: Application to the Synthesis of the Taxol and Bestatin Side Chains and Related Systems. *Tetrahedron Lett.* **1990**, *31*, 6429–6432.
- (a) *Recent Progress in the Chemical Synthesis of Antibiotics*; Lukacs, G., Ohno, M., Eds.; Springer-Verlag: Berlin, 1990; pp 565–612. (b) Nagahara, T.; Kametani, T. Enantioselective Syntheses of Carbapenem Antibiotics. *Heterocycles* **1987**, *25*, 729–806.
- The Chemistry of  $\beta$ -lactams*; Page, M. I., Ed.; Chapman Hall: New York, 1992.
- Staudinger, M. Zur Kenntniss der Ketene. *Liebigs Ann. Chem.* **1907**, *356*, 51–123.
- Buynak, J. D.; Rao, M. N.  $\alpha$ -Alkylidene- $\beta$ -Lactams. A Formal Synthesis of ( $\pm$ )-Carpetimycin A. *J. Org. Chem.* **1986**, *51*, 1571–1574.
- Buynak, J. D.; Rao, M. N.; Pajouhesh, H.; Chandrasekaran, R. Y.; Finn, K.; de Meester, P.; Chu, S. C. Useful Chemistry of 3-(1-Methylethylidene)-4-acetoxy-2-azetidinone: A Formal Synthesis of ( $\pm$ )-Asparenomycin C. *J. Org. Chem.* **1985**, *50*, 4245–4252.
- (a) Buynak, J. D.; Mathew, J.; Rao, M. N. A Formal Synthesis of ( $\pm$ )-Thienamycin. *J. Chem. Soc., Chem. Commun.* **1986**, 941–942. (b) Johnston, D. B. R.; Schmitt, S. M.; Bouffard, F. A.; Christensen, B. G. Total synthesis of ( $\pm$ )-thienamycin. *J. Am. Chem. Soc.* **1978**, *100*, 313–315.
- Moriconi, E. J.; Kelly, J. F. The stereospecific cycloaddition of chlorosulfonyl isocyanate to *cis*- and *trans*- $\beta$ -methylstyrene and *cis*- and *trans*-3-hexene. *Tetrahedron Lett.* **1968**, 1439.
- Paquette, L. A.; Kakahama, T.; Hansen, J. F.; Philips, J. C. Unsaturated heterocyclic systems. LXXIII. P-equivalent heterocyclic congeners of cyclooctatetraene. Synthesis and valence isomerization of 2-alkoxyazocines. *J. Am. Chem. Soc.* **1971**, *93*, 152–161.
- Moriconi, E. J.; Meyer, W. C. Reaction of dienes with chlorosulfonyl isocyanates. *J. Org. Chem.* **1971**, *36*, 2841–2849.
- Chmielewski, M.; Kaluza, Z.; Belzecki, C.; Salański, S.; Jurczak, J.; Adamowicz, M. High-pressure (2+2) cycloaddition of toluene-4-sulphonyl isocyanate to glycals. *Tetrahedron* **1985**, *41*, 2441–2449.
- Cossio, F. P.; Lecea, B.; Lopez, X.; Roa, G.; Arrieta, A.; Ugalde, J. M. An Ab Initio study on the mechanism of alkene-isocyanate cycloaddition reaction to form  $\beta$ -lactams. *J. Chem. Soc., Chem. Commun.* **1993**, 1450–1452.
- Cossio, F. P.; Roa, G.; Lecea, B.; Ugalde, J. M. Substituent and Solvent Effects in the [2 + 2] Cycloaddition Reaction between Olefines and Isocyanates. *J. Am. Chem. Soc.* **1995**, *117*, 12306–12313.
- Rode, J. R.; Dobrowolski, J. Cz.; Borowiak, M. A.; Mazurek, A. P. A theoretical study on the stability and spectra of cycloaddition products: Methylene- $\beta$ -lactam isomers. *Phys. Chem. Chem. Phys.* **2002**, *4*, 3948–3958.
- Moore, H. W.; Hughes, G.; Srinivasachar, K.; Fernández, M.; Nguyen, N. V.; Schoon, D.; Tranne, A. Cycloadditions of cyanoketenes to cinnamylidenamines and benzylidenamines. Synthetic scope, stereochemistry, and mechanism. *J. Org. Chem.* **1985**, *50*, 4231–4238.
- (a) Pacansky, J.; Chang, J. S.; Brown, D. W.; Schwarz, W. Observation of Zwitterions in the Thermal Reaction of Ketenes with Carbon–Nitrogen Double Bonds. *J. Org. Chem.* **1982**, *47*, 2233–2234. (b) Lynch, J. E.; Riseman, S. M.; Laswell, W. L.; Tschäen, D. M.; Volante, R. P.; Smith, G. B.; Shinkai, I. Mechanism of an Acid Chloride–Imine Reaction by Low-Temperature FTIR:  $\beta$ -Lactam Formation Occurs Exclusively through a Ketene Intermediate. *J. Org. Chem.* **1989**, *54*, 3792–3796.
- (a) Sordo, J. A.; Gonzales, J.; Sordo, T. L. An Ab Initio Study on the Mechanism of the Ketene–Imine Cycloaddition Reaction. *J. Am. Chem. Soc.* **1992**, *114*, 6249–6251. (b) Cossio, F. P.; Ugalde, J. M.; Lopez, X.; Lecea, B.; Palomo, C. A semiempirical theoretical study on the formation of  $\beta$ -lactams from ketenes and imines. *J. Am. Chem. Soc.* **1993**, *115*, 995–1004.
- (a) Assfeld, X.; Ruiz-Lopez, M. F.; Gonzalez, J.; Lopez, R.; Sordo, J. A.; Sordo, T. L. Theoretical Analysis of the Role of the Solvent on the Reaction mechanism: One-Step versus Two-Step Ketene–Imine Cycloadd-

- dition. *J. Comput. Chem.* **1994**, *15*, 479–487. (b) Truong, T. H. Solvent effects on structure and reaction mechanism: a theoretical study of [2 + 2] polar cycloaddition between ketene and imine. *J. Phys. Chem. B* **1998**, *102*, 7877–7881.
- (30) Barbaro, G.; Battaglia, A.; Giorgianni, P. 2-Iminooxetane chemistry. 2. General Synthesis from ketene imine–aldehyde cycloadditions. *J. Org. Chem.* **1988**, *53*, 5501–5506.
- (31) (a) Mori, M.; Kagechika, K.; Tohjima, K.; Shibasaki, M. New Synthesis of 4-acetoxy-2-azetidiones by Use of Electrochemical Oxidation. *Tetrahedron Lett.* **1988**, *29*, 1409–1412. (b) Mori, M.; Ban, Y. Debenzylation of N-benzyl- $\beta$ -Lactams by use of Anodic Oxidation. *Heterocycles* **1985**, *23*, 317–323.
- (32) Dejaegher, Y.; Kuz'menok, N. M.; Zvonok, A. M.; De Kimpe, N. The chemistry of azetid-3-ones, oxetan-3-ones, thietan-3-ones. *Chem. Rev.* **2002**, *102*, 29–60.
- (33) (a) Ubukata, M.; Uramato, M.; Uzawa, J.; Isono, K. Structure and biological activity of neopeptins A, B, and C, inhibitors of fungal cell wall glycan synthesis. *Agric. Biol. Chem.* **1986**, *50*, 357. (b) Ludwig, E.; Lyr, H.; Kluge, E.; Uhlemann, E.; Zanke, D. Ger. (East) Pat. 1980, 140,838 (Cl. A01N37/18), 2nd April 1980 Appl. 210017, 21st December 1978; 23 pp, Fungicidal composition; *Chem. Abstr.* **1981**, *94*, 151877h. (c) Foguet Ambros, R.; Forne Felip, E.; Ortiz Hernández, J. A.; Sacristan Munoz, A. 1,2-oxazetidines (Ferver International SA) Spanish Patent 1984, 519,297 (Cl. C07D413/12) 1st March 1984, Appl. 19th January 1983, 7 pp; *Chem. Abstr.* **1985**, *103*, 123468. (d) Magers, D. H.; Davis, S. R. Ring strain in the oxazetidines. *J. Mol. Struct. (THEOCHEM)* **1999**, *487*, 205–210. (e) Fabian, W. M. F. Semiempirical AM1 and PM3 Calculations on the peri-, site-, and Regiochemistry of Heterocumulene-Heterodiene Cycloadditions. *Acta Chim. Acad. Sci. Hung.* **1992**, *129*, 347–355.
- (34) (a) Perna, F.; Capriati, V.; Florio, S.; Luisi, R. Isomerization of oxazolin allylic alcohols: synthesis of 3-alkilidene-2-iminooxetanes. *Tetrahedron Lett.* **2003**, *44*, 3477–3481. (b) Barbaro, G.; Battaglia, A.; Giorgianni, P. 2-Iminooxetane chemistry. 2. General Synthesis from ketene imine–aldehyde cycloadditions. *J. Org. Chem.* **1988**, *53*, 5501–5506. (c) Barbaro, G.; Battaglia, A.; Giorgianni, P. 2-Iminooxetane chemistry. 3. Synthesis of  $\beta$ -hydroxy Amides. *J. Org. Chem.* **1992**, *57*, 5128–5136. (d) Barbaro, G.; Battaglia, A.; Giorgianni, P.; Giacomini, D. Cyclocondensation Reactions of Optically Active  $\alpha$ -alkoxy aldehydes to ketene imines: Synthesis of Chiral 2-Iminooxetanes. *Tetrahedron* **1993**, *49*, 4293–4306.
- (35) (a) Bothe, E.; Dessouki, A. M.; Schulte-Frohlinde, D. Rate and Mechanism of the Ketene Hydrolysis in Aqueous Solution. *J. Phys. Chem.* **1980**, *84*, 3270–3272. (b) Skancke, P. N. Theoretical Study of the Hydration Reaction of Ketene. *J. Phys. Chem.* **1992**, *96*, 8065–8069. (c) Frey, J.; Rappoport, Z. Reversibility of Ketene Hydration. *J. Am. Chem. Soc.* **1995**, *117*, 1161–1162. (d) Duan, X.; Page, M. Theoretical Investigation of Competing Mechanisms in the Thermal Unimolecular Decomposition of Acetic Acid and the Hydration Reaction of Ketene. *J. Am. Chem. Soc.* **1995**, *117*, 5114–5119. (e) Nguyen, M. T.; Raspoet, G. The hydration of ketene: 15 years later. *Can. J. Chem.* **1999**, *77*, 817–829.
- (36) (a) Aigner, M.; Zeilinger, M.; Hofbauer, H. Kinetic study of the hydrolysis of isocyanic acid in the gas phase. *Chem. Eng. Process.* **1995**, *34*, 515–520. (b) Raunier, S.; Chiaavassa, T.; Allouche, A.; Marinelli, F.; Aycaud, J. P. Thermal reactivity of HNCO with water ice: an infrared and theoretical study. *Chem. Phys.* **2003**, *288*, 197–210. (c) Raunier, S.; Chiaavassa, T.; Marinelli, F.; Aycaud, J. P. Experimental and theoretical study on the spontaneous formation of OCN<sup>-</sup> ion: reactivity between HNCO and NH<sub>3</sub>/H<sub>2</sub>O environment at low temperature. *Chem. Phys.* **2004**, *302*, 259–264.
- (37) Møller, C.; Plesset, M. S. Note on an Approximation Treatment for Many-Electron Systems. *Phys. Rev.* **1934**, *46*, 618–622.
- (38) (a) Woon, D. E.; Dunning, T. H., Jr. Gaussian basis sets for use in correlated molecular calculations. III. The atoms aluminum through argon. *J. Chem. Phys.* **1993**, *98*, 1358–1371. (b) Kendall, R. A.; Dunning, T. H., Jr.; Harrison, R. J. Electron affinities of the first-row atoms revisited. Systematic basis sets and wave functions. *J. Chem. Phys.* **1992**, *96*, 6796–6806.
- (39) Zhao, Y.; Pu, J.; Lynch, B. J.; Truhlar, D. G. Tests of second-generation and third-generation density functionals for thermochemical kinetics. *Phys. Chem. Chem. Phys.* **2004**, *6*, 673–676.
- (40) Peng, C.; Schlegel, H. B. Combining Synchronous Transit and Quasi-Newton Methods to Find Transition States. *Isr. J. Chem.* **1993**, *33*, 449–454.
- (41) Peng, C.; Ayala, P. Y.; Schlegel, H. B.; Frisch, M. J. Using Redundant Internal Coordinates to Optimize Equilibrium Geometries and Transition States. *J. Comput. Chem.* **1996**, *17*, 49–56.
- (42) (a) Cancès, M. T.; Mennucci, B.; Tomasi, J. A new integral equation formalism for the polarizable continuum model: Theoretical background and applications to isotropic and anisotropic dielectrics. *J. Chem. Phys.* **1997**, *107*, 3032–3041. (b) Mennucci, B.; Tomasi, J. Continuum solvation models: A new approach to the problem of solute's charge distribution and cavity boundaries. *J. Chem. Phys.* **1997**, *106*, 5151–5058. (c) Cossi, M.; Barone, V.; Mennucci, B.; Tomasi, J. Ab initio study of ionic solutions by a polarizable continuum dielectric model. *Chem. Phys. Lett.* **1998**, *286*, 253–260. (d) Cossi, M.; Scalmani, G.; Rega, N.; Barone, V. New developments in the polarizable continuum model for quantum mechanical and classical calculations on molecules in solution. *J. Chem. Phys.* **2002**, *117*, 43–54.
- (43) (a) Gonzales, C.; Schlegel, H. B. An improved algorithm for reaction path following. *J. Chem. Phys.* **1989**, *90*, 2154–2161. (b) Gonzales, C.; Schlegel, H. B. Reaction path following in mass-weighted internal coordinates. *J. Phys. Chem.* **1990**, *94*, 5523–5527.
- (44) Breneman, C. M.; Wiberg, K. B. Determining atom-centered monopoles from molecular electrostatic potentials. The need for high sampling density in formamide conformational analysis. *J. Comput. Chem.* **1990**, *11*, 361–373.
- (45) Frisch, M. J.; Trucks, G. W.; Schlegel, H. B.; Scuseria, G. E.; Robb, M. A.; Cheeseman, J. R.; Zakrzewski, V. G.; Montgomery, J. A.; Stratmann, R. E.; Burant, J. C.; Dapprich, S.; Milliam, J. M.; Daniels, A. D.; Kudin, K. N.; Strain, M. C.; Farkas, O.; Tomasi, J.; Barone, V.; Cossi, M.; Cammi, R.; Mennucci, B.; Pomelli, C.; Adamo, C.; Clifford, S.; Ochterski, J.; Petersson, G. A.; Ayala, P. Y.; Cui, Q.; Morokuma, K.; Malick, D. K.; Rabuck, A. D.; Raghavachari, K.; Foresman, J. B.; Cioslowski, J.; Ortiz, J. V.; Stefanov, B. B.; Liu, G.; Liashenko, A.; Piskorz, P.; Komaromi, I.; Gomperts, R.; Martin, R. L.; Fox, D. J.; Keith, T. A.; Al-Laham, M. A.; Peng, C. Y.; Nanayakkara, A.; Gonzales, C.; Challacombe, M.; Gill, P. M. W.; Johnson, B. G.; Chen, W.; Wong, M. W.; Andres, J. L.; Replogle, E. S.; Head-Gordon, M.; Replogle, E. S.; Pople, J. A. *Gaussian 98*, revision A.7; Gaussian, Inc.: Pittsburgh, PA, 1998.
- (46) Frisch, M. J.; Trucks, G. W.; Schlegel, H. B.; Scuseria, G. E.; Robb, M. A.; Cheeseman, J. R.; Montgomery, J. A., Jr.; Vreven, T.; Kudin, K. N.; Burant, J. C.; Millam, J. M.; Iyengar, S. S.; Tomasi, J.; Barone, V.; Mennucci, B.; Cossi, M.; Scalmani, G.; Rega, N.; Petersson, G. A.; Nakatsuji, H.; Hada, M.; Ehara, M.; Toyota, K.; Fukuda, R.; Hasegawa, J.; Ishida, M.; Nakajima, T.; Honda, Y.; Kitao, O.; Nakai, H.; Klene, M.; Li, X.; Knox, J. E.; Hratchian, H. P.; Cross, J. B.; Bakken, V.; Adamo, C.; Jaramillo, J.; Gomperts, R.; Stratmann, R. E.; Yazyev, O.; Austin, A. J.; Cammi, R.; Pomelli, C.; Ochterski, J. W.; Ayala, P. Y.; Morokuma, K.; Voth, G. A.; Salvador, P.; Dannenberg, J. J.; Zakrzewski, V. G.; Dapprich, S.; Daniels, A. D.; Strain, M. C.; Farkas, O.; Malick, D. K.; Rabuck, A. D.; Raghavachari, K.; Foresman, J. B.; Ortiz, J. V.; Cui, Q.; Baboul, A. G.; Clifford, S.; Cioslowski, J.; Stefanov, B. B.; Liu, G.; Liashenko, A.; Piskorz, P.; Komaromi, I.; Martin, R. L.; Fox, D. J.; Keith, T.; Al-Laham, M. A.; Peng, C. Y.; Nanayakkara, A.; Challacombe, M.; Gill, P. M. W.; Johnson, B.; Chen, W.; Wong, M. W.; Gonzalez, C.; Pople, J. A. *Gaussian 03*, revision C.2; Gaussian, Inc.: Wallingford, CT, 2004.
- (47) Flükiger, P.; Lüthi, H. P.; Portmann, S.; Weber, J. *MOLEKEL 4.0*; Swiss Centre for Scientific Computing: Manno, Switzerland, 2000.
- (48) (a) Biegler-König, F.; Schönbohm, J. *AIM2000, A Program to Analyze and Visualize Atoms in Molecules*, version 2.0. (b) Bader, R. F. W. *Atoms in Molecules: A Quantum Theory*; Clarendon Press: Oxford, U.K., 1990.
- (49) Fukui, K. Role of frontier orbitals in chemical reactions. *Science* **1981**, *218*, 747–754.
- (50) Jean, Y.; Volatron, F. *An Introduction to Molecular Orbitals*; Oxford University Press, New York, 1993.
- (51) Tomasi, J.; Mennucci, B.; Cammi, R. Quantum Mechanical Continuum Solvation Models. *Chem. Rev.* **2005**, *105*, 2999–3094.
- (52) (a) Woodward, R. B.; Hoffmann, R. The Conservation of Orbital Symmetry. *Angew. Chem., Int. Ed. Engl.* **1969**, *8*, 781–932. (b) Woodward, R. B.; Hoffmann, R. *The Conservation of Orbital Symmetry*; Verlag Chemie: Weinheim, Germany, 1970.
- (53) Bernardi, F.; Bottoni, A.; Olivucci, M.; Robb, M. A.; Schlegel, H. B.; Tonachini, G. Do Supra-Antra Paths Exist for 2 + 2 Cycloaddition Reactions? Analytical Computation of the MC-SCF Hessians for Transition States of C<sub>2</sub>H<sub>2</sub> with C<sub>2</sub>H<sub>2</sub>, Singlet O<sub>2</sub>, and Ketene. *J. Am. Chem. Soc.* **1988**, *110*, 5993–5995.
- (54) (a) Birney, D. M.; Wagenseller, P. E. An ab Initio Study of the Reactivity of Formylketene. Pseudopericyclic Reactions Revisited. *J. Am. Chem. Soc.* **1994**, *116*, 6262–6270. (b) Birney, D. M.; Ham, S.; Unruh, G. R. Pericyclic and Pseudopericyclic Thermal Chelotropic Decarbonylations: When Can a Pericyclic Reaction Have a Planar, Pseudopericyclic Transition State? *J. Am. Chem. Soc.* **1997**, *119*, 4509–4517. (c) Birney, D. M. Electrocylic Ring Openings of 2-Furylcarbene and Related Carbenes: A Comparison between Pseudopericyclic and Concerted Reactions. *J. Am. Chem. Soc.* **2000**, *122*, 10917–10925. (d) Shumway, W.; Ham, S.; Moer, J.; Whittlesey, B. R.; Birney, D. M. Felkin-Anh Stereoselectivity in Cycloadditions of Acetylketene: Evidence for a Concerted, Pseudopericyclic Pathway. *J. Org. Chem.* **2000**, *65*, 7731–7739. (e) Zhou, C.; Birney, D. M. A Density Functional Theory Study Clarifying the Reactions of Conjugated Ketenes with Formaldimine. A Plethora of Pericyclic and Pseudopericyclic Pathways. *J. Am. Chem. Soc.* **2002**, *124*, 5231–5241. (f) Wei, H.-X.; Zhou, C.; Ham, S.; White, J. M.; Birney, D. M. Experimental Support for Planar Pseudopericyclic Transition States in Thermal Chelotropic Decarbonylations. *Org. Lett.* **2004**, *6*, 4289–4292.
- (55) (a) Fabian, W. M. F.; Bakulev, V. A.; Kappe, C. O. Pericyclic vs Pseudopericyclic 1,5-Electrocyclization of Iminodiazomethanes. An ab Initio

and Density Functional Theory Study. *J. Org. Chem.* **1998**, *63*, 5801–5805. (b) Fabian, W. M. F.; Kappe, C. O.; Bakulev, V. A. Ab Initio and Density Functional Calculations on the Pericyclic vs Pseudopericyclic Mode of Conjugated Nitrile Ylide 1,5-Electrocyclizations. *J. Org. Chem.* **2000**, *65*, 47–53. (c) Fukushima, K.; Iwahashi, H. Natural Bond Orbital Analysis of Pericyclic and Pseudopericyclic 1,5-Electrocyclizations of Conjugated Nitrileimines. *Bull. Chem. Soc. Jpn.* **2004**, *77*, 1671–1679.

(56) Cabaleiro-Lago, E. M.; Rodríguez-Otero, J.; Hermida-Ramón, J. Evaluation of Magnetic Properties as a Criterion for the Elucidation of the Pseudopericyclic Character of 1,5-Electrocyclizations in Nitrile Ylides. *J. Phys. Chem. A* **2003**, *107*, 4962–4966.

(57) (a) Rodríguez-Otero, J.; Cabaleiro-Lago, E. M.; Hermida-Ramón, J.; Peña-Gallego, A. DFT Study of Pericyclic and Pseudopericyclic Thermal Chelotropic Decarbonylations. Evaluation of Magnetic Properties. *J. Org. Chem.* **2003**, *68*, 8823–8830. (b) Montero-Campillo, M. M.; Rodríguez-Otero, J.; Cabaleiro-Lago, E. M. Ab Initio and DFT Study of the Reaction Mechanism of Diformylketene with Formamide. *J. Phys. Chem.* **2004**, *108*, 8373–8377. (c) Peña-Gallego, A.; Rodríguez-Otero, J.; Cabaleiro-Lago, E. M. A DFT Study of the Boulton-Katritzky Rearrangement of (5*R*)-4-Nitrosobenz[c]isoxazole and Its Anion: Pseudopericyclic Reactions with Aromatic Transition States. *J. Org. Chem.* **2004**, *69*, 7013–7017. (d) Cabaleiro-Lago, E. M.; Rodríguez-Otero, J.; González-López, I.; Peña-Gallego, A.; Hermida-Ramón, J. A DFT Study of the Pericyclic/Pseudopericyclic Character of Cycloaddition Reactions of Ethylene and Formaldehyde to Buta-1,3-dien-1-one and Derivatives. *J. Phys. Chem. A* **2005**, *109*, 5636–5644.

(58) Chamorro, E. The nature of bonding in pericyclic and pseudopericyclic transition states: Thermal chelotropic decarbonylations. *J. Chem. Phys.* **2003**, *118*, 8687–8698.

(59) (a) Ross, J. A.; Seiders, R. P.; Lemal, D. M. An Extraordinary Facile Sufoxide Automerization. *J. Am. Chem. Soc.* **1976**, *98*, 4325–4327.

(b) Bushweller, C. H.; Ross, J. A.; Lemal, D. M. Autoimerization of a Dewar Thiophene and Its *exo*-*S*-Oxide. A Dramatic Contrast. *J. Am. Chem. Soc.* **1977**, *99*, 629–631.

(60) Silva López, C.; Nieto Faza, O.; Cossio, F. P.; York, D. M.; de Lera, A. R. Ellipticity: A Convenient Tool To Characterize Electrocyclic Reactions. *Chem.–Eur. J.* **2005**, *11*, 1734–1738.

(61) Gilchrist, T. L.; Storr, R. C. *Organic Reactions and Orbital Symmetry*, 2nd ed.; Cambridge University Press: New York, 1979.

(62) (a) Salzner, U.; Bachrach, S. M. Ab Initio Studies of the Dimerization of Ketene and Phosphaketene. *J. Am. Chem. Soc.* **1994**, *116*, 6850–6855.

(b) Seidl, E. T.; Schaefer, H. F., III. Theoretical Investigations of the Dimerization of Ketene: Does the 2S + 2A Cycloaddition Reaction Exist? *J. Am. Chem. Soc.* **1991**, *113*, 5195–5200. (c) Jug, K.; Chickos, J.

Mechanistic Pathways for Ketene Dimerization. *Theor. Chim. Acta* **1975**, *40*, 207–219. (d) Jug, K.; Dwivedi, C. P. D. Reaction Pathways for Various Ketene Dimers. *Theor. Chim. Acta* **1978**, *90*, 249–257. (e) Fu, X. Y.; Decai, F.; Yanbo, D. Theoretical Studies on the Reaction Mechanism of Ketene

Dimerization Reactions. *J. Mol. Struct. (THEOCHEM)* **1988**, *167*, 349–358. (f) Seidl, E. T.; Schaefer, H. F., III. Theoretical Investigations of the Dimerization of Ketene: Does the 2S + 2A Cycloaddition Reaction Exist? *J. Am. Chem. Soc.* **1991**, *113*, 5195–5200. (g) Salzner, U.; Bachrach, S. M. Ab Initio Studies of the Dimerization of Ketene and Phosphaketene. *J. Am. Chem. Soc.* **1994**, *116*, 6850–6855. (h) Carless, H. J., *Photochemistry in Organic Synthesis*; Coyte, J. D., Ed.; Royal Society of Chemistry: London, 1986; p 95. (i) Zimmerman, H. E. *Pericyclic Reactions*; Marchand, A. P., Lehr, R. E., Eds.; Academic Press: New York, 1977.

(63) (a) Sadlej-Sosnowska, N.; Dobrowolski, J. Cz.; Oziminski, W.; Mazurek, A. P. On the conformation and hydrogen bonding in the vigabatrin amino acid. *J. Phys. Chem. A* **2002**, *106*, 10554–10562. (b) Wojtulewski, S.; Grabowski, S. J. Ab initio and AIM studies on intramolecular dihydrogen

bonds. *J. Mol. Struct.* **2002**, *645*, 287–294.